

ATMOSPHERIC CARBON DIOXIDE AND ITS RELATION TO CARBON
CYCLE PERTURBATIONS DURING OCEAN ANOXIC EVENT 1D: A
HIGH RESOLUTION RECORD FROM DISPERSED PLANT CUTICLE

by

Jon Daniel Richey, B.S.

A thesis submitted to the Graduate Council of
Texas State University in partial fulfillment
of the requirements for the degree of
Master of Science
with a Major in Biology
August 2014

Committee Members:

Garland R. Upchurch, Jr., Chair

David E. Lemke

Noland H. Martin

Marina B. Suarez

COPYRIGHT

by

Jon Daniel Richey

2014

FAIR USE AND AUTHOR'S PERMISSION STATEMENT

Fair Use

This work is protected by the Copyright Laws of the United States (Public Law 94-553, section 107). Consistent with fair use as defined in the Copyright Laws, brief quotations, from this material are allowed with proper acknowledgement. Use of this material for financial gain without the author's express written permission is not allowed.

Duplication Permission

As the copyright holder of this work I, Jon Daniel Richey, authorize duplication of this work, in whole or in part, for educational or scholarly purposes only.

DEDICATION

For my wife, Adrienne, and our daughter, Evangeline Ruth.

ACKNOWLEDGEMENTS

I want to express my deepest appreciation to Dr. Garland Upchurch for his mentoring and the help I needed to complete this work. Throughout our five years together as student and advisor, you taught me how to think like a scientist and prepared me for my future.

I would like to thank the other members of my committee, Dr. David Lemke, Dr. Noland Martin, and Dr. Marina B. Suarez, for their help and guidance. I would like to thank Dr. Suarez in particular for the use of her facilities at University of Texas at San Antonio.

I thank Dr. Matt Joeckel, Dr. Greg Ludvigson, and Dr. John Smith for arranging access to the Rose Creek Locality and measuring the section during the hottest August Nebraska has ever seen. This work would not have been possible without your help.

I thank the Deboer family for access to the Rose Creek Pit locality.

I would like to thank Dr. Barry Lomax for many useful discussions, help with this project, and use of his facilities at the University of Nottingham. You have always been available to help no matter what the situation and I appreciate it.

I would like to thank my current and former labmates (Dr. Emilio Estrada-Ruiz, Joan Parrott, Dori Contreras, Barroq Safi, Adam Bilsing, Patricia Valella, and Jacquelyn Scherer) for being the kind of people who make it enjoyable to work in the lab when I

could be swimming in the San Marcos River. Having a great group of people around to converse with on a day-to-day basis helped me grow as a researcher.

I also thank the Texas State Department of Biology, The Texas State Graduate College, and the National Science Foundation for their support, financial or otherwise.

I thank my friends and family for being a constant source of help and encouragement.

Finally, I thank my wife, Adrienne Richey, for providing the encouragement I needed to complete this task and withstanding the worst of my ever-changing, thesis-related moods.

Grant and fellowship funding for this work: National Science Foundation Graduate Research Fellowship (\$32,000), Texas State University Graduate College Thesis Support Fellowship (\$2,000)

Disclaimer: This material is based upon work supported by the National Science Foundation Graduate Research Fellowship under Grant No. DGE-1144466. Any opinion, findings, and conclusions or recommendations expressed in this material are those of the author and do not necessarily reflect the views of the National Science Foundation.

This manuscript was submitted to my thesis committee for final review on June 12th, 2014. Final version, with revisions suggested by my thesis committee, was submitted to the Texas State Graduate College on July 14th, 2014.

TABLE OF CONTENTS

	Page
ACKNOWLEDGEMENTS	v
LIST OF FIGURES	viii
LIST OF ABBREVIATIONS.....	ix
ABSTRACT	xi
CHAPTER	
I. INTRODUCTION.....	1
Goals of This Study	1
Ocean Anoxic Events.....	2
Ocean Anoxic Event 1d	7
Stomatal Index	11
Fossil Charcoal, Vitrain, and Carbon Isotopes	16
The Rose Creek Pit, Southeastern Nebraska.....	23
II. MATERIALS AND METHODS.....	30
III. RESULTS	39
Geochemistry	39
Stomatal Index and CO ₂	44
IV. DISCUSSION.....	49
LITERATURE CITED	58

LIST OF FIGURES

Figure	Page
1. The Rose Creek Pit, Southeastern Nebraska.....	24
2. The Eastern Margin of the Western Interior Seaway, Middle Cretaceous	25
3. Lower Section at the Rose Creek Pit, 2012	26
4. Upper Section at the Rose Creek Pit, 2012.....	27
5. Comparison of the Lower and Upper Sections of This Study and the Lower and Upper Sections of Gröcke et al. (2006)	31
6. Species Used in Stomatal Index Analysis.....	34
7. <i>Pandemophyllum</i> Morphotypes Used in Stomatal Index Analysis.....	35
8. Chemostratigraphy of the Rose Creek Pit Area, Compared to Wilson and Norris (2001).....	40
9. Carbon Isotopes and Stomatal Index from Rose Creek Pit, Southeastern Nebraska	45
10. Carbon Isotopes and pCO ₂ From Rose Creek Pit, Southeastern Nebraska	47

LIST OF ABBREVIATIONS

Abbreviation	Description
OAE(s)	Ocean Anoxic Event(s)
SI	Stomatal Index
pCO ₂	Partial pressure of carbon dioxide
OAE1a	Ocean Anoxic Event 1a
OAE1b	Ocean Anoxic Event 1b
OAE1c	Ocean Anoxic Event 1c
OAE1d	Ocean Anoxic Event 1d
OAE2	Ocean Anoxic Event 2
OAE3	Ocean Anoxic Event 3
ACB	Albian-Cenomanian Boundary
TOAE	Toarcian Ocean Anoxic Event
GHG(s)	Greenhouse gas(es)
LIP	Large Igneous Province
P-OAE	Productivity Ocean Anoxic Event
D-OAE	Detritus Ocean Anoxic Event
forams	foraminifera
TOC	Total organic content
SD	Stomatal Density

WUE	Water Use Efficiency
<i>HIC</i>	High Carbon Dioxide
$\delta^{13}\text{C}_{\text{plant}}$	$\delta^{13}\text{C}$ of plants
$\delta^{13}\text{C}_{\text{atm}}$	$\delta^{13}\text{C}$ of the atmosphere
RuBisCo	Ribulose 1, 5 bisphosphate carboxylase/oxygenase
$\delta^{13}\text{C}_{\text{char}}$	$\delta^{13}\text{C}$ of charcoal
PAH(s)	Polyaromatic hydrocarbons
$\delta^{13}\text{C}_{\text{coal}}$	$\delta^{13}\text{C}$ of coal
$\delta^{13}\text{C}_{\text{org}}$	$\delta^{13}\text{C}$ of organic matter
$\delta^{13}\text{C}_{\text{wood}}$	$\delta^{13}\text{C}$ of wood
$\delta^{13}\text{C}_{\text{carb}}$	$\delta^{13}\text{C}$ of carbonate
RCP	Rose Creek Pit
WIS	Western Interior Seaway
$\delta^{13}\text{C}_{\text{bulk}}$	$\delta^{13}\text{C}$ of bulk organics
$\delta^{13}\text{C}_{\text{foram}}$	$\delta^{13}\text{C}$ of foraminifera
RCP UC	Rose Creek Pit Upper Core
SD	Standard Deviation
$\delta^{13}\text{C}_{\text{gym}}$	$\delta^{13}\text{C}$ of gymnosperm charcoal
$\delta^{13}\text{C}_{\text{vit}}$	$\delta^{13}\text{C}$ of vitrain
Myr	millions of years

ABSTRACT

Past geological greenhouse intervals are associated with Ocean Anoxic Events (OAEs), which result from an increase in marine primary productivity and/or an increase in the preservation of organic matter. The end point is widespread black shale deposition in the deep ocean combined with a long-term atmospheric positive $\delta^{13}\text{C}$ excursion and an increase in the burial of ^{12}C . Some OAEs show a negative $\delta^{13}\text{C}$ excursion preceding the positive excursion, indicating a perturbation in the global carbon cycle prior to the initiation of these events.

The Rose Creek Pit (RCP) locality, southeastern Nebraska, is currently the only known terrestrial section that preserves OAE1d (Cretaceous, Albian-Cenomanian Boundary) and has abundant charcoal and plant cuticle. These features allow for a combined analysis of carbon isotopes and stomatal index (SI) to determine changes in the cycling between carbon pools (carbon isotope analysis) and their relation to paleo- CO_2 via changes in SI. To do this, RCP SI data were calculated from the cuticle of *Pandemophyllum kvacekii* (an extinct laurel) and related taxa, and fitted to $\delta^{13}\text{C}$ curves derived from fossil gymnosperm charcoal and vitrain, as well as other published charcoal and bulk organic $\delta^{13}\text{C}$ profiles from RCP and nearby sediment cores. Absolute values of CO_2 were estimated using three published transfer functions based on species of extant Lauraceae. This study represents the first attempt to quantify variation in CO_2 during OAE1d.

SI indicates changes in CO_2 coincident with changes in $\delta^{13}\text{C}$. Pre-excursion pCO_2 was relatively low (330–615 ppm) and was associated with a slight positive shift in $\delta^{13}\text{C}$ (~1‰) immediately preceding the negative excursion recorded in other RCP $\delta^{13}\text{C}$ curves. Those curves record a negative excursion (avg. $\approx 2.21\text{‰}$) beginning at or slightly below the floor of RCP. This study records a more modest negative shift of $\sim 1.2\text{--}1.47\text{‰}$ because sampling began after the beginning of the negative excursion. All RCP chemostratigraphy shows that negative excursion lasts through ~ 3.3 m of the section.

During this negative excursion, pCO₂ increases from the pre-excursion values to a high of ~380–800 ppm. After the negative excursion, all RCP chemostratigraphic curves and pCO₂ values show a slow return to pre-excursion values. Despite the finer sampling intervals of this study compared to others at RCP and in surrounding areas, fossil gymnosperm charcoal and vitrain δ¹³C curves do not record the positive excursion found in foraminifera and carbonate δ¹³C curves during OAE1d. This study confirms that δ¹³C of fossil wood, whether coalified or charcoaled, and SI from dispersed cuticle can reliably capture carbon cycle perturbations and changes in atmospheric CO₂ around OAEs.

I. INTRODUCTION

Goals of This Study

Ocean Anoxic Events (OAEs) are global climate cycle perturbations. The current injection of massive amounts of carbon dioxide (CO₂) and methane (CH₄) due to anthropogenic activities is analogous in some ways to natural perturbations in the carbon cycle such as OAEs. Evidence for this is seen in the current negative carbon isotopic excursion attributed to anthropogenic CO₂ emissions (IPCC, 2007). Atmospheric CO₂, and presumably global temperatures, are expected to reach levels not seen since the greenhouse climates of the Cretaceous, during which OAEs were a relatively common occurrence (Beerling et al., 1993; Leckie et al., 2002; Montanez et al., 2011; Pachauri and Reisinger, 2007). In addition, modern oceans have anoxic areas that have grown exponentially in the past 50 years (Diaz and Rosenberg, 2008). While changes in atmospheric CO₂ have been quantified during other OAEs (Barclay et al., 2010; McElwain et al., 2005), it has never been inspected using fine sampling intervals, which will allow detailed comparisons of changes in atmospheric CO₂ and the carbon cycle. This is essential to understanding the nature and climatic tipping points of GHG-initiated OAEs. My master's research is designed to evaluate this relationship by reconstructing changes in partial pressure of CO₂ (pCO₂) during OAE1d using Stomatal Index (SI).

With this study, I address three questions. First, can the carbon isotope excursion found in analysis of fossil charcoal and bulk organics by Gröcke et al. (2006) and Gröcke and Joeckel (2008) be reproduced using new collections of fossil charcoal and vitrain? Second, if the carbon isotope excursion can be reproduced, what was the pattern of

changes in atmospheric CO₂ during the perturbation? Finally, if there is a discernable pattern of change in atmospheric CO₂, how does the change compare to CO₂ changes found during OAEs by other researchers (Barclay et al., 2010; McElwain et al., 2005). My study is one of the few studies to use SI to reconstruct atmospheric CO₂ during a major perturbation of the global carbon cycle. It is also the first to use SI to reconstruct changes in atmospheric CO₂ during Ocean Anoxic Event 1d (OAE1d), which has been subject to less study than other OAEs. The questions I will attempt to answer about OAE1d will add to our knowledge of these events in general.

Ocean Anoxic Events

During the early days of exploration of deep ocean sediments, extremely organic carbon-rich sediments of Cretaceous age were recovered in the Indian, Atlantic, and Pacific oceans. Schlanger and Jenkyns (1976) correlated these organic-rich black shales with coeval Tethyan deposits in the Caribbean and Mediterranean regions, among others, suggesting widespread to global distribution. In addition, these sediments contained sapropelic markers such as pyrite, glauconite, phosphate, and dolomite, similar to well-studied Mediterranean sapropelic sediments attributed to anoxia due to limited local oceanic circulation (Erbacher et al., 2001; Schlanger and Jenkyns, 1976; Wilson and Norris, 2001). Because of the global nature of organic carbon-rich sediments throughout the Aptian-Albian and Cenomanian-Turonian stages, Schlanger and Jenkyns (1976) named these events Ocean Anoxic Events.

At least nine OAEs have been documented for the Cretaceous (Arthur et al., 1990; Jenkyns, 2010; Leckie et al., 2002; Takashima et al., 2006). They are: 1) Weissert Event

(Late Valanginian) (Erba et al., 2004), 2) Faraoni Event (Latest Hauterivian) (Baudin, 2005), 3) OAE1a (Selli Event, Early Aptian), 4) OAE1b (Paquier Event, Aptian-Albian Boundary), 5) OAE1c (Toolebuc Event, Late Albian), 6) OAE1d (Breistroffer Event, Albian-Cenomanian Boundary [ACB]) (Arthur et al., 1990; Erbacher and Thurow, 1997; Schlanger and Jenkyns, 1976), 7) Mid-Cenomanian Event (Coccioni and Galeotti, 2003), 8) OAE2 (Bonarelli Event, Cenomanian-Turonian Boundary) (Schlanger and Jenkyns, 1976), and 9) OAE3 (Coniacian-Santonian Boundary) (Jenkyns, 1980). While most common during the greenhouse climate of the Cretaceous, OAEs are not restricted to that period. Other OAEs include the Mid-Proterozoic (Arnold et al., 2004), Ordovician-Silurian Boundary, Devonian (Kellwasser Event) (Joachimski and Buggisch, 1993), Early Mississippian (Meyer and Kump, 2008), Jurassic (Posidonienschiefer Event, Toarcian; also known as the TOAE) (Jenkyns, 1988), the Cretaceous-Tertiary (K-T) Boundary (Kajiwara and Kaiho, 1992) and the Paleocene-Eocene Thermal Maximum (Jenkyns, 2010; Sluijs et al., 2006). Of the major Mesozoic OAEs, TOAE, OAE1a, and OAE2 are considered global in nature (Erba, 2004; Jenkyns, 2010; Leckie et al., 2002). Researchers disagree about the global vs. regional significance of remaining Cretaceous OAEs. OAE1b, OAE1c, and OAE1d are considered to have regional, but still widespread, significance by some (Erba, 2004), while others consider OAE1b and OAE1d to be global events (Jenkyns, 2010).

Most OAEs are marked by long-term (10^4 – 10^6 years) positive $\delta^{13}\text{C}$ excursions due to the increased burial of organic ^{12}C -enriched sediments as black shales. There has been significant disagreement as to the cause of black shale deposition (Arthur et al., 1990; Pedersen and Calvert, 1990). Depending on the researcher, black shales are the

result of either an increase in marine primary productivity or an increase in preservation of organic material due to ocean anoxia and/or stagnation, or by some combination of the two mechanisms (Arthur et al., 1988; Erbacher et al., 2005; Hochuli et al., 1999).

Increased primary productivity is now thought to be the most important causal factor in black shale development (Erba, 2004; Jenkyns, 2010). Massive sequestration of large amounts of carbon in marine organisms and, ultimately, black shales leads to reduction in dissolved oceanic carbon dioxide (CO₂). This causes increased flux of CO₂ to the oceans and a drawdown of atmospheric CO₂ (Arthur et al., 1988; Barclay et al., 2010; Hochuli et al., 1999; Kuypers et al., 1999; McElwain et al., 2005; Stoll and Schrag, 2000; Weissert et al., 1998).

Schlanger and Jenkyns (1976) originally proposed a two-step cause for OAE1 and OAE2. First, marine transgression caused inundation of coastal plains and deltas, washing large amounts of plant organic matter into the ocean, as well as increasing the extent and volume of shallow seas with high marine primary productivity. In modern oceans, regions of extremely high organic productivity are found in the Mediterranean and continental shelves. The ratio of these conditions to the entire ocean is 1:30 (Sverdrup et al., 1942). During the mid-Cretaceous, at the height of marine transgression, this ratio was 1:6, indicating that levels of organic carbon in oceans were much higher in the Cretaceous than modern oceans (Hays and Pitman, 1973; Jenkyns, 1980; Schlanger and Jenkyns, 1976). Second, the existence of worldwide warm, equable climate caused a disruption in oceanic circulation, which led to a decrease in influx of cold oxygenated water from polar regions (Schlanger and Jenkyns, 1976).

Other researchers have implicated greenhouse gases (GHG) and climatic warming

via volcanism as the primary causal factor in the initiation of Cretaceous OAEs. The simplest evidence for this is that these events are characteristic of “greenhouse” climates of the geologic past (Jenkyns, 2003). Furthermore, most Cretaceous OAEs are clustered in the Aptian-Turonian stages, which coincide with the formation of many Large Igneous Provinces (LIPs), instances of increased sea-floor spreading and hydrothermal vent activity, and/or an increase in crust production in general (Barclay et al., 2010; Erba, 2004; Jenkyns, 2003; Jones and Jenkyns, 2001; Kuroda et al., 2007; Larson and Erba, 1999; Leckie et al., 2002; Takashima et al., 2006; Turgeon and Creaser, 2008). In these GHG-initiated events, the injection of isotopically light carbon (CO₂ or methane [CH₄]) causes a pronounced, but relatively short-lived (10³–10⁴ years) negative δ¹³C excursion preceding the positive isotope excursion. Other evidence of initiation of some OAEs by volcanism is a decrease in ⁸⁷Sr/⁸⁶Sr, ¹⁸⁷Os/¹⁸⁸Os, and an increase in trace metal concentration (Jones and Jenkyns, 2001). Other OAEs are thought to have GHG origins by other mechanisms, such as the massive injection of CO₂ and CH₄ to the atmosphere from the release of methane hydrates from the deep ocean (Erba, 2004; Hesselbo et al., 2000; Jahren et al., 2001), or massive injection of CH₄ to the atmosphere from the intrusion of magma into organic-rich sediments (specifically coals) (McElwain et al., 2005; Svenson et al., 2004).

A number of climate/volcanism-related secondary causes for OAEs have been proposed, including an increased hydrologic cycle, which, in turn, would cause increased continental weathering and enhanced nutrient discharge to oceans and lakes and increased upwelling of nutrient-rich waters (Menegatti et al., 1998). Heimhoffer et al. (2006) have argued that an increased hydrologic cycle would lead to significant addition

of terrestrial organic matter to the oceans. Others have implicated trace metal fertilization from marine volcanism in increased marine productivity (Larson and Erba, 1999). In line with the original hypothesis of Schlanger and Jenkyns (1976), some researchers have cited marine transgression as the causal factor in OAEs (Arthur and Sageman, 1994; Erbacher et al., 1996). Conversely, in some cases, marine regression is cited as a cause (Erbacher et al., 1996). Finally, changes in oceanic stratification and circulation have been shown to have a role in ocean anoxia (Erbacher et al., 2001; Watkins et al., 2005; Wilson and Norris, 2001).

An important consequence of OAEs is their effect on marine organisms. The mid-Cretaceous, the time when most OAEs cluster, was also a time of major turnover in marine plankton, benthic foraminifera (forams), and mollusks (Leckie et al., 2002). Ocean Anoxic Events, in particular, are times of relative maxima of turnover of marine organisms. Erbacher et al. (1996) expanded upon the causes of Cretaceous OAEs and their effects on marine organisms by placing each into one of two categories.

One type is termed P-OAEs (P = productivity). These events are characterized by marine transgression, the presence of positive $\delta^{13}\text{C}$ excursions, heightened marine productivity and significant marine turnover. Erbacher et al. (1996) hypothesized that during these events, transgression caused leaching of nutrients from recently inundated coastal land, causing an explosion in aerobic marine productivity. The increased oxygen demand would expand the oxygen-minimum zone, causing extinction of radiolarians and forams. Evidence of this is seen in the high occurrence of type II (marine planktonic) kerogen in the black shales of P-OAEs. As the oxygen-minimum zones shrank to their normal bounds, radiation of new species would begin to fill the ecological niches

(Erbacher et al., 1996). Using these criteria, Erbacher et al. (1996) classified OAE1a, OAE1b, OAE1d, the Mid-Cenomanian Event, and OAE2 as P-OAEs. This classification has been verified by other researchers who found major marine turnover clustered around the OAEs listed above (Erba, 2004; Leckie et al., 2002; Watkins et al., 2005).

The second type of OAE is characterized by marine regression, the lack of positive isotopic excursion, no increased marine productivity, and radiolarian radiations. In addition, this type of OAE is characterized by black shale containing type III (humic) kerogen, indicative of addition of large amounts of terrigenous organic matter (presumably plant matter) to the ocean (Pratt and King, 1986). Because of this, Erbacher et al. (1996) named this type of event D-OAE (D = Detritus). Only one Cretaceous OAE (OAE1c) is categorized as a D-OAE. In terms of marine organisms, the continual fall in sea levels during OAE1c caused a shortage of nutrients, stimulating an extinction event. This has been verified by other researchers, who have found significant radiolarian speciation around OAE1c (Leckie et al., 2002).

Ocean Anoxic Event 1d

Ocean Anoxic Event 1d (Breistroffer Event) is a time of widespread to global deposition of marine organic matter as black shales at the ACB (Wilson and Norris, 2001). Sediments that preserve this event occur in southeast France, (Bornemann et al., 2005; Br  h  ret, 1994; Br  h  ret and Delamette, 1989; Breistroffer, 1937; Gale et al., 1996; Giraud et al., 2003), central and northern Italy (Erbacher et al., 1996; Stoll and Schrag, 2000), Switzerland (Strasser et al., 2001), Spain (L  pez-Horgue et al., 1999), Japan (Ando and Kakegawa, 2007; Kawabe et al., 2003), California (Robinson et al.,

2008), New Mexico (Scott et al., 2013), south and northeast Texas (Phelps, 2012; Reichelt, 2005), southeast Nebraska (Gröcke and Joeckel, 2008; Gröcke et al., 2006), the Atlantic Ocean (Hofmann et al., 2000; Leckie et al., 2002; Nederbragt et al., 2001; Petrizzo et al., 2008; Watkins et al., 2005; Wilson and Norris, 2001), and the Pacific Ocean (Thiede et al., 1981). Ocean Anoxic Event 1d is an interval of carbonaceous mudstone to black shale deposition, with an organic carbon content of up to ~25% by weight (/wt.) in some marine sections (Hofmann et al., 2000; Wilson and Norris, 2001). OAE1d occurred, in part, during a time of eustatic lowering of global sea levels (Haq et al., 1987; Haq and Schutter, 2008).

Wilson and Norris (2001) used $\delta^{18}\text{O}$ of surface and thermocline-dwelling forams with known depth habitats isolated in pelagic marine carbonate to propose a possible cause for OAE1d. Due to the fractionation of oxygen isotopes related to temperature, $\delta^{18}\text{O}$ can be used to infer paleotemperature in deep time. There is also a consistent offset in $\delta^{18}\text{O}$ values of surface and thermocline-dwelling foram species due to depth-habitat temperature. At the beginning of OAE1d black shale deposition, the $\delta^{18}\text{O}$ curves of surface and thermocline dwelling species of foram converge. This result supports the “high productivity” model for black shale deposition, as the “increased preservation/stagnation” model invokes increased salinity and temperature stratification as a cause (Erbacher et al., 2001). In addition, the $\delta^{18}\text{O}$ of the surface dwelling forams give an Atlantic sea surface temperature 3–5 °C warmer than today, most likely the result of GHG forcing (Wilson and Norris, 2001). These data led Wilson and Norris (2001) to conclude that OAE1d was a time of global black shale development caused by climatic warming, increased marine productivity, and a collapse of the upper ocean water column

stratification due to a combination of increased of winter mixing and decreased summer stratification. However, some challenge the global aspect and role of productivity of this event, due to: 1) evidence of time-equivalent oxic sediments in other parts of the Atlantic, 2) time-equivalent sediments only slightly enriched in organic carbon, and 3) evidence of a modest increase in fertility during the event (Giraud et al., 2003; Hofmann et al., 2000; López-Horgue et al., 1999; Nederbragt et al., 2001; Scott et al., 2013).

Ocean Anoxic Event 1d has been the subject to detailed carbon isotope stratigraphy in planktonic forams (Wilson and Norris, 2001), bulk rock/marine carbonate (Bornemann et al., 2005; Erbacher and Thurow, 1997; Erbacher et al., 1996; Leckie et al., 2002; Nederbragt et al., 2001; Phelps, 2012; Reichelt, 2005; Robinson et al., 2008; Stoll and Schrag, 2000; Strasser et al., 2001; Watkins et al., 2005), bulk organics (Ando and Kakegawa, 2007; Gröcke and Joeckel, 2008; Gröcke et al., 2006; Scott et al., 2013), and fossil charcoal (Ando and Kakegawa, 2007; Gröcke et al., 2006). Though considerable variability exists between OAE1d $\delta^{13}\text{C}$ curves, most of the curves show large positive excursions ($\sim.5\text{--}2\text{‰}$), marking deposition of organic-rich black shales (Bornemann et al., 2005; Erbacher et al., 1996; Leckie et al., 2002; Nederbragt et al., 2001; Reichelt, 2005; Robinson et al., 2008; Scott et al., 2013; Stoll and Schrag, 2000; Strasser et al., 2001; Watkins et al., 2005; Wilson and Norris, 2001). Though detailed estimates of CO_2 during OAE1d are non-existent, there is evidence of rapid climatic cooling (relative to the hot climate of the mid-Cretaceous as a whole) from the $\delta^{18}\text{O}$ paleothermometer at the ACB, implying a drawdown in atmospheric CO_2 (Clarke and Jenkyns, 1999; Kawabe et al., 2003; Stoll and Schrag, 2000). Several of the OAE1d $\delta^{13}\text{C}$ curves listed above show a pronounced negative excursion ($\sim.5\text{--}3\text{‰}$) (Bornemann et al., 2005; Gröcke and

Joeckel, 2008; Gröcke et al., 2006; Phelps, 2012; Reichelt, 2005; Watkins et al., 2005; Wilson and Norris, 2001), indicative of a release of isotopically light carbon. Some of the $\delta^{13}\text{C}$ curves show both the positive and negative excursion associated with OAE1d (Bornemann et al., 2005; Reichelt, 2005; Watkins et al., 2005; Wilson and Norris, 2001). In addition, several show many smaller negative and positive excursions around the largest “main” negative and positive excursions, indicating possible multiple instances of isotopically light carbon release and deposition (Bornemann et al., 2005; Gröcke and Joeckel, 2008; Gröcke et al., 2006; Watkins et al., 2005; Wilson and Norris, 2001).

Ocean Anoxic Event 1d also represents a time of major turnover in radiolarians (Erbacher and Thurow, 1997; Erbacher et al., 1996), planktonic forams (Leckie et al., 2002), and calcareous nannoplankton (Watkins et al., 2005), with species-level extinction of radiolarian and planktonic forams estimated to be 23–30% and 26–28%, respectively. This is confirmed by reports of large amounts of marine organic matter (type II kerogen) in OAE1d black shales (total organic content [TOC] up to ~25% /wt., commonly .5–2.5% /wt.) (Bréhéret, 1994; Bréhéret and Delamette, 1989; Erbacher et al., 1996; Wilson and Norris, 2001). This is consistent with the hypothesis of heightened marine productivity during OAEs, and, in combination with the positive isotope excursion, led to OAE1d being designated a P-OAE.

However, several researchers report a significant amount of terrigenous organic matter (type III kerogen) in individual black shales (Bornemann et al., 2005; Hofmann et al., 2000; Scott et al., 2013). Interestingly, the occurrence of terrigenous organic matter is highly variable between localities. In some cases it is a constant significant portion of the TOC throughout OAE1d, while in others the amount of terrigenous organic matter

peaks during black shales and drops off after, and in others it is the dominant form of organic matter throughout. In all cases, the studied sections are near-shore marine and the common hypothesis for the terrigenous content of organic matter is either an increase hydrologic cycle or marine transgression. If the terrigenous content of black shale organic matter is indicative of transgression, then OAE1d has all the characteristics of a P-OAE. However, OAE1d is hypothesized to coincide with a eustatic lowering of global sea levels, which Erbacher et al. (1996) evoked to explain the occurrence of terrigenous organic matter during D-OAEs (Haq et al., 1987; Haq and Schutter, 2008). Despite this, OAE1d is usually described as a P-OAE due to the inferred increase in productivity during the event.

Stomatal Index

E. J. Salisbury's classic (1928) paper was the first analysis of the effect environmental factors on the number of stomata (gas exchange pores of the leaves of plants). In this paper, he measured stomatal density,

$$(SD) = \frac{\# \text{ stomata}}{\text{mm}^2} \quad [1],$$

in leaves of differing type, size, position on the parent plant, and under various water and light availabilities. In addition, he looked at intra-leaf variation in SD. He found that all variables had an effect on SD, with the exception of light availability. However, he noted that differences in SD could be due to a greater number of stomata or by variation in the size of non-specialized epidermal cells. In order to eliminate the effect of epidermal cell size from his analysis of stomatal frequency, Salisbury (1928) formally proposed a new measure, Stomatal Index,

$$(SI) = \left[\frac{S}{S+E} \right] * 100 \quad [2],$$

where S is the number of stomata and E is the number of epidermal cells excluding guard cells. Using SI, Salisbury (1928) found that variation in stomatal frequency under experimental parameters was due to changes in epidermal cell size, rather than changes in stomatal number.

The connection between stomatal frequency and atmospheric CO₂ was not established until Woodward (1987) compared SI (Eq. 2) and SD (Eq. 1) of various modern woody deciduous species with herbarium specimens collected during the Industrial Revolution and its resulting increase in CO₂. He found that plants show a decrease in SI (Eq. 2) and SD (Eq. 1) with increasing CO₂ levels, indicating that CO₂ levels (at least partially) control stomatal initiation in order to maximize Water Use Efficiency ([WUE], the ratio of photosynthesis and transpiration) (Woodward, 1987, 1993). Woodward (1987) hypothesized that this relationship exists because, at high CO₂ levels, an individual leaf can maintain its rate of carbon uptake while reducing water loss by having fewer stomata. Likewise, at lower atmospheric CO₂ levels, an individual leaf increases the number of stomata to maintain the rate of carbon assimilation, at the expense of increased transpiration (e.g. Royer, 2001).

Recent research suggests that the SI/CO₂ relationship in plants has a genetic component and is the product of long distance signaling from mature leaves to developing leaves. Developing leaves show reduced SD and SI as a result of exposing mature leaves contained within air-tight cuvettes to elevated CO₂ (Lake et al., 2001; Lake et al., 2002; Miyazawa et al., 2006). In addition, Gray et al. (2011) identified the gene *HIC* (= High Carbon Dioxide) in *Arabidopsis* which codes for a negative regulator that

responds to CO₂ levels, and Ferris et al. (2002) found quantitative trait loci that control the SI/CO₂ relationship in species of *Populus*.

The SI response of plants to changes in CO₂ is species specific (Royer, 2001) and non-linear at high CO₂ levels (Kürschner et al., 2008; Royer et al., 2001). Stomatal Index is insensitive to local environmental factors, such as irradiance (Kürschner, 1997; Poole et al., 1996; Salisbury, 1928; Sharma and Dunn, 1968, 1969; Wagner, 1998), water availability/humidity (Clifford et al., 1995; Estiarte et al., 1994; Salisbury, 1928; Sharma and Dunn, 1968, 1969), position of leaf in the forest canopy (Royer, 2001; Salisbury, 1928), and habitat, as well as other factors such as woodiness, stature, and ploidy level (Rowson, 1943; Woodward and Kelly, 1995). Temperature has been shown to have an effect on both SD and SI by some (Ferris et al., 1996; Wagner, 1998), and no effect on SI by others (Reddy et al., 1998). However, most plants mitigate the effect of temperature fluctuation by adjustment of the timing of leaf development, possibly negating the effect on stomatal initiation (Wagner, 1998). The apparent insensitivity of SI (vs. SD and other measures) to confounding environmental factors makes SI a powerful tool for deep time studies where such factors are unknown.

The inverse relation of SI and atmospheric CO₂ proposed by Woodward (1987) has been corroborated by many different methods. The relation has been observed by the growth of modern plants in sealed chambers at various levels of increased CO₂ (Barclay et al., 2010; Beerling et al., 1998; Beerling and Woodward, 1995, 1997; Carpenter, 2005; Ceulemans et al., 1995; Clifford et al., 1995; Haworth et al., 2011; Kürschner et al., 1998; Lomax, 2001; Malone et al., 1993; Thomas and Harvey, 1983; Woodward, 1986; Woodward and Bazzaz, 1988). In addition, the relation has been verified by the

comparison of SI in subfossil material, including, 1) collected leaves and plants growing close to a CO₂ spring (Beerling and Woodward, 1997; Jones et al., 1995), 2) cored leaf material from a single tree or several trees growing in an aquatic environment with high preservation (Kouwenberg et al., 2003; Rundgren and Beerling, 1999; van Hoof et al., 2006; Wagner et al., 1996; Wagner et al., 2005), and 3) herbarium specimens (Greenwood et al., 2003; Kouwenberg et al., 2003; Kürschner, 1996; Kürschner et al., 1996; McElwain et al., 1995; Penuelas and Matamala, 1990; Van Der Burgh et al., 1993; van Hoof et al., 2006; Wagner et al., 2005) with known CO₂ levels measured at the Mauna Loa observatory (Wagner et al., 1996) and in ice core samples (Friedli et al., 1986; Indermühle et al., 1999; Kouwenberg et al., 2003; Kürschner, 1996; Kürschner et al., 1996; McElwain et al., 1995; Neftel et al., 1985; Penuelas and Matamala, 1990; Rundgren and Beerling, 1999; Van Der Burgh et al., 1993). Finally, the relationship has been verified by comparison of modern SI measurements with Salisbury's (1928) SI calculations (Beerling and Kelly, 1997).

Studies that utilize SI in the deep geologic past are also common due to the relative insensitivity of SI to all parameters beside CO₂. However, extant plants have been exposed to CO₂ levels of 180–280 ppm over the last 800,000+ years (Petit et al., 1999). Therefore, SI studies have often utilized plants grown in chambers at elevated CO₂. These data are combined with data from herbarium specimens to make stomatal response curves, from which transfer functions are derived. Stomatal Index from the cuticle of fossil plants is plugged into a transfer function for their closest living relative to estimate paleo-CO₂. Using this method, researchers have used SI to reconstruct atmospheric pCO₂ in the Holocene (Beerling et al., 1992; McElwain et al., 1995; Rundgren and Beerling,

1999; Wagner et al., 1999), Pleistocene (Beerling et al., 1993; Van Der Burgh et al., 1993), Pliocene (Kürschner, 1996; Kürschner et al., 1996; Van Der Burgh et al., 1993), Miocene (Kürschner et al., 2008), Eocene (Greenwood et al., 2003; McElwain, 1998), across the Cretaceous-Tertiary Boundary (Beerling et al., 2002b), Cretaceous (Barclay et al., 2010; Chen et al., 2001; Haworth et al., 2005; Passalia, 2009; Quan et al., 2009; Retallack, 2009; Wan et al., 2011), Jurassic (McElwain, 1998; McElwain and Chaloner, 1996; McElwain et al., 2005; Retallack, 2009), the Jurassic-Triassic Boundary (McElwain et al., 1999; Steinthorsdottir et al., 2011), Permian (McElwain and Chaloner, 1995; Retallack, 2009), Pennsylvanian (Cleal et al., 1999), and Devonian (Edwards et al., 1998; McElwain and Chaloner, 1995).

Though *Ginkgo* and *Metasequoia* have often been used in deep time SI studies due to their status as “living fossils” (Royer, 2003), Lauraceae are a plant family with strong potential for reconstructing changes in atmospheric CO₂ during the Cretaceous. Lauraceae could rival those plants’ utility, being present in most Late Cretaceous leaf assemblages from the middle latitudes. In addition, the climatic tolerances of Lauraceae (subtropical to tropical) are a much better match to the warm to hot climates of the Cretaceous than the climatic tolerances of *Ginkgo* and *Metasequoia* (temperate). Barclay et al. (2010) used transfer functions derived from extant lauraceous species (*Laurus nobilis* and *Hypodaphnis zenkeri*) to reconstruct pCO₂ levels for comparison to δ¹³C around OAE2, which marks the Cenomanian-Turonian Boundary. They found that the positive δ¹³C excursions of OAE2 were accompanied by dramatic, synchronous decreases in atmospheric pCO₂. In addition, Kürschner et al (2008) used transfer functions derived from SI in the extant lauraceous species *L. nobilis* and *Ocotea foetens*

and the fossil Lauraceous species *Laurophyllum pseudoprinceps* to reconstruct pCO₂ in the Miocene. I have used fossil Lauraceae and the transfer functions of Barclay et al. (2010) to reconstruct atmospheric CO₂ levels for intervals of the Late Cretaceous and found a similar decline inferred by other proxy methods (Richey, 2011; Royer, 2010). These studies showed the potential for the use of fossil Lauraceae in the estimation of pCO₂ levels and interpretation of OAEs.

Fossil Charcoal, Vitrain, and Carbon Isotopes

Many factors control the carbon isotopic composition of C₃ plants (trees, shrubs forbs, lianas, and some grasses). First and foremost, the δ¹³C of plants (δ¹³C_{plant}) is controlled by the isotopic composition of the atmosphere (Recent δ¹³C_{atm} ≈ -8.0‰, pre-Industrial Revolution ≈ -7‰), the source of CO₂ for photosynthesis. Second, it is controlled by the discrimination against the heavier carbon isotope, in the form of ¹³CO₂, during C₃ photosynthesis. Farquhar (1989) derived the following equation to describe the discrimination (Δ) against the carbon 13 in plants,

$$\Delta = a + (b - a) \frac{p_i}{p_a} \quad [3],$$

where a is the fractionation ([Δδ] during the diffusion of CO₂ in air through the stomatal pore (Δδ ≈ 4.4‰) (Farquhar, 1983), the diffusion of CO₂ in air through the boundary layer to the stomatal pore (Δδ ≈ 2.9‰) (O'Leary, 1981), and the diffusion of dissolved CO₂ through the aqueous cellular environment of photosynthetic cells (Δδ ≈ 0.7‰) (O'Leary, 1984), b is the second, stronger, fractionation during the addition of CO₂ to ribulose 1,5 biphosphate by the enzyme ribulose 1,5 biphosphate carboxylase/oxygenase (RuBisCo), which discriminates against ¹³CO₂ for kinetic reasons (Δδ ≈ 30.0‰) (Roeske

and O'Leary, 1984), and p_i/p_a is the ratio of intercellular $p\text{CO}_2$ to $p\text{CO}_2$ surrounding an individual leaf (note: this term is commonly expressed as concentrations (c_i/c_a) instead of pressure) (Farquhar et al., 1989; O'Leary, 1981). With unlimited CO_2 , enzymatic fractionation is the only factor affecting $\delta^{13}\text{C}_{\text{plant}}$, and C_3 plants would have a $\delta^{13}\text{C}_{\text{plant}} \approx -37\text{‰}$ (Hoefs, 2009; Michener and Lajtha, 2008; O'Leary, 1981). With CO_2 as a limiting factor, diffusion of CO_2 into leaves plays more important role in fractionation, and $\delta^{13}\text{C}_{\text{plant}}$ increases to its observed range for C_3 of -23‰ – -34‰ (avg. = -27‰) (Farquhar and Richards, 1984; Smith and Epstein, 1971).

Other factors that can cause variation in $\delta^{13}\text{C}_{\text{plant}}$ of C_3 biomass, such as species (Ehleringer et al., 1987), latitude/altitude (Bird et al., 1996; Bird et al., 1994; Körner et al., 1991), precipitation/humidity/soil water deficit (Lipp et al., 1991; Stewart et al., 1995), topographic position (Balesdent et al., 1993), salinity (Guy et al., 1980), and use of recycled (i.e. respired) CO_2 in closed forest canopies (Broadmeadow et al., 1992; Graham and Freeman, 2013; Van der Merwe and Medina, 1989; Vogel, 1978) (Bird and Ascough, 2012; Gröcke, 1998). In addition, there can be considerable variation in $\delta^{13}\text{C}$ within an individual plant. There are significant differences between the dominant components of wood, with cellulose being isotopically heavier than whole plant tissue by 1‰ – 2‰ and lignin being isotopically lighter than whole plant tissue by 2‰ – 6‰ (Benner et al., 1987). There is also variation between leaves and wood (3‰ – 4‰), leaves of an individual plant (up to 4‰) (Leavitt and Long, 1991), twigs and branches (2‰ – 3‰) (Leavitt and Long, 1986), and early wood and late wood (1‰ – 2‰) (Leavitt and Long, 1982).

There are also changes in the carbon isotopic composition of wood during the

process of charcoalfication. Charcoal (i.e. fusain in the fossil record and inertinite as a component of coal) is the product of the incomplete combustion of plants and is indicative of wildfire (Scott, 1989, 2010; Scott and Glasspool, 2007). Though oxygen (O_2) is inherently necessary for wildfires to form, charcoal is formed in a relative lack of O_2 (pyrolysis) (Pyne et al., 1996; Scott and Jones, 1991b). This paradoxical relationship is due to the nature of plant tissue, which contains little to no O_2 . While the outer plant tissue layers combust, heat penetrates the low O_2 environment of the plant interior, breaking down cellulose and releasing carbon monoxide (CO), CO_2 , and CH_4 , which in turn, combust, feeding the fire (Pyne et al., 1996). If this reaction ends before complete combustion can occur, charcoal is produced. The remaining charcoal shows characteristic cracking, often appearing as 1 cm^3 cubes that are relatively inert and easily preserved in the fossil record, depending on depositional environment and other factors (see following paragraphs) (Scott, 2000; Scott and Glasspool, 2007; Scott and Jones, 1991a). Charcoal fragments are brittle, have a splintery/powdery fracture, are lustrous, and preserve the anatomy of the parent plant material, allowing them to be identified down to the genus and species level (Scott, 2001, 2010).

The average change in $\delta^{13}C$ during charcoalfication is $+0.36\text{‰}$ -1.24‰ , with changes of up to $\pm 2.0\text{‰}$ reported (Ascough et al., 2008; Bird and Gröcke, 1997; Cachier et al., 1985; Czimczik et al., 2002; Ferrio et al., 2006; Jones and Chaloner, 1991; Jones et al., 1993; Krull et al., 2003; Leavitt et al., 1982; McParland et al., 2007; Poole et al., 2002; Turney et al., 2006). There are observable patterns in changes in $\delta^{13}C$ of charcoal ($\delta^{13}C_{\text{char}}$) with increasing temperature during formation. There is an initially an enrichment in $\delta^{13}C_{\text{char}}$ values up to $\sim 100\text{ }^\circ\text{C}$, attributed to the loss of isotopically light

minor wood elements and/or the physical trapping of isotopically heavy cellulose carbon within the charcoal structure (Czimczik et al., 2002; Hakkou et al., 2006; Jones et al., 1993; Poole et al., 2002). Up to $\sim 300^{\circ}\text{C}$, $\delta^{13}\text{C}_{\text{char}}$ decreases by 1–2‰ due to the preferential loss of isotopically heavy cellulose, which is much less thermally stable than lignin (Ascough et al., 2008; Benner et al., 1987; Bird and Gröcke, 1997; Cachier et al., 1985; Czimczik et al., 2002; DeNiro and Hastorf, 1985; Jones and Chaloner, 1991; Jones et al., 1993; Loader et al., 2003; Maunu, 2002; Turney et al., 2006; Williams and Besler, 1996; Xiao et al., 2001). During the preceding temperature changes, the carbon content of charcoal increases, while O_2 and hydrogen content decreases due to the breakdown of lignin and cellulose and formation of aromatic carbon rings (Bird and Ascough, 2012). Above $\sim 400^{\circ}\text{C}$, polyaromatic hydrocarbons (PAHs) are formed, which eventually form ordered microcrystalline structures that are chemically stable and highly decay resistant (especially in anoxic environments) (Czimczik et al., 2005; Eckmeier et al., 2007; Masiello, 2004; Preston and Schmidt, 2006). Some researchers suggest a further depletion of $\delta^{13}\text{C}_{\text{char}}$ during the formation of carbon double bonds in PAHs, though the magnitude of the depletion has not been quantified (Krull et al., 2003; Qian et al., 1992).

The studies listed above also indicate that O_2 levels affect $\delta^{13}\text{C}_{\text{char}}$. They found significant differences in $\delta^{13}\text{C}_{\text{char}}$ produced in “natural” fires vs. charcoal produced in a vacuum. The lower $\delta^{13}\text{C}$ of vacuum-produced charcoal is attributed to the accelerated loss of cellulose during formation (Krull et al., 2003; Leavitt et al., 1982; Turney et al., 2006). There is also evidence of differing effects of oxygen levels depending on starting material. For example, Ascough et al. (2008) reported that O_2 levels affected the $\delta^{13}\text{C}$ of gymnosperm charcoal (*Pinus sylvestris*), while angiosperm charcoal (*Rhizophora*

apiculata) was unaffected.

Though charcoal has been reported to be highly stable and decay resistant (Czimczik et al., 2005; Preston and Schmidt, 2006), oxidative weathering in the post-depositional environment can play a significant role in some cases, either by the addition of oxygen to aromatic rings in PAHs or by addition of carboxylic (COOH- and COO-) groups to PAHs (Ascough et al., 2008; Cohen-Ofri et al., 2006). This effect can be extreme, such that it can affect the overall abundance of charcoal in some localities. For example, some archeological sites, where cooking and other fires were known to occur, show a complete loss of all charcoal over a few millennia (Bird et al., 2002), while other sites show a reduction in charcoal abundance in as few as 50 years (Bird et al., 1999).

Vitrain (or vitrinite) is coalified plant material (Scott, 2010; Taylor et al., 1998). Vitrain is an important (and most abundant) component (maceral) of coal (Scott, 2002). Vitrain fragments are generally 1 mm³ in size, have a bright luster, conchoidal fracture, and, when broken, have a glassy appearance in which no anatomy of the parent plant material can be seen (Scott, 2010). The transformation of wood to vitrain begins in the peat stage, where cellulose is preferentially degraded until completely gone and lignin is preferentially preserved (Hatcher and Clifford, 1997). From there, many chemical changes occur in the remaining lignin, such as dehydroxylation, alkylation, and demethylation, among others, as the plant material moves from lignite rank to sub-bituminous rank (Hatcher and Clifford, 1997). In addition, during the peatification process, anaerobic bacteria-mediated alteration and recombination of humic material causes woody material to become gelified (Bechtel et al., 2004; Bechtel et al., 2003). This gel fills the intracellular spaces of the plant material (Scott, 2002). When the plant

material reaches the sub-bituminous rank, cellular structure is no longer visible and the material has the characteristic glassy appearance of vitrain (Hatcher et al., 1994; Scott, 2002).

While much work has been done on carbon isotopes of coal, little work has been done in relation to $\delta^{13}\text{C}$ of specific coal macerals (Rimmer et al., 2006). Because, like charcoal, vitrain is derived from plant material, it is subject to all of the factors that affect the $\delta^{13}\text{C}$ of plants (listed in detail earlier in this section). The carbon isotopic composition of coals ($\delta^{13}\text{C}_{\text{coal}}$) range from -22 to -27‰ , which falls within range reported (-23 to -34‰) for C_3 vegetation (Gröcke, 1998; Rimmer et al., 2006; Whiticar, 1996). Rimmer et al. (2006) performed carbon isotope analysis on vitrain-rich coal fractions and found an average value of -23.5‰ , which falls in the range for fossil plants (-23 to -27‰) and C_3 vegetation. However, the preferential loss of isotopically heavy cellulose and gellification by anaerobic bacteria (through bacterial carbon recycling) should theoretically make the value of vitrain isotopically light (Bechtel et al., 2004; Bechtel et al., 2003; Rimmer et al., 2006).

Rimmer et al. (2006) also performed carbon isotope analysis on inertinite-rich coal fractions and generated an average of -23‰ . This result agrees with that of Whiticar (1996), who found that inertinite is slightly isotopically heavier than vitrain, and that of Jones et al. (1993), who found that fusain was isotopically heavier than vitrain by 0.8 – 2‰ . It also agrees with the slight positive shift at low temperatures seen the charring experiments discussed in detail above (Czimeczik et al., 2002; Hakkou et al., 2006; Poole et al., 2002). Despite this, other researchers have stated that there is little systemic difference between coalified and charcoalified wood (Hesselbo et al., 2000; Hesselbo et

al., 2003).

Scholle and Arthur (1980) were the first researchers to suggest that $\delta^{13}\text{C}$ excursions recorded in marine carbonate could be communicated to land plants through changes in $\delta^{13}\text{C}_{\text{atm}}$. The $\delta^{13}\text{C}$ of dissolved inorganic (oceanic) carbon is thought to be related to the partitioning of global carbon between oxidized (CO_2 /carbonate/bicarbonate) and reduced (organic) carbon (Gröcke et al., 1999). Therefore, the burial of excess isotopically-light organic carbon causes a positive excursion in $\delta^{13}\text{C}$ and a drawdown of atmospheric CO_2 , as stated previously. Decreased dissolved and atmospheric CO_2 levels would lead to a decrease in fractionation in organic matter and a positive shift in $\delta^{13}\text{C}$ of organics ($\delta^{13}\text{C}_{\text{org}}$) and wood ($\delta^{13}\text{C}_{\text{wood}}$). The two factors listed above (partial pressure and $\delta^{13}\text{C}$ of atmospheric CO_2) work in concert to make isotopic shifts in both marine and terrestrial organic matter larger than those found in carbonate (Gröcke et al., 1999). In addition, since atmospheric CO_2 levels are affected by other factors (rates of weathering, depositional rate of calcium carbonate [CaCO_3], volcanism), shifts in $\delta^{13}\text{C}_{\text{org}}$ and carbonate isotope ($\delta^{13}\text{C}_{\text{carb}}$) curves may not be in phase with each other (Arthur et al., 1988; Arthur et al., 1985; Lini et al., 1992).

Despite the sources of variation in $\delta^{13}\text{C}_{\text{org}}$ listed above, changes in $\delta^{13}\text{C}_{\text{org}}$ (bulk organics, fossil wood, coalified wood, charcoal/fusain/inertinite, vitrain/vitrinite cuticle, etc.) have been correlated to changes in $\delta^{13}\text{C}_{\text{carb}}$ at the Triassic-Jurassic Boundary (Hesselbo et al., 2002), in the Middle Jurassic (Hesselbo et al., 2003), Toarcian (Hesselbo et al., 2000), Early Cretaceous (Gröcke, 1997; Gröcke et al., 2005; Jahren et al., 2001; Robinson and Hesselbo, 2004), Aptian through Albian (Ando and Kakegawa, 2007; Ando et al., 2002, 2003; Gröcke et al., 1999; Heimhofer et al., 2003), the ACB (Ando and

Kakegawa, 2007; Gröcke and Joeckel, 2008; Gröcke et al., 2006; Scott et al., 2013), the Cenomanian-Turonian Boundary (Hasegawa, 1997), the Late Cretaceous (Hasegawa et al., 2003), the Paleocene-Eocene Boundary (Koch et al., 1992; Stott et al., 1996), and throughout the geologic past (Beerling and Royer, 2002). Most of the examples listed above are studies of OAEs. All $\delta^{13}\text{C}_{\text{org}}$ curves show the same isotopic excursions seen in $\delta^{13}\text{C}_{\text{carb}}$ with a few exceptions. As hypothesized, excursions in $\delta^{13}\text{C}_{\text{org}}$ are often much larger and/or out of phase with $\delta^{13}\text{C}_{\text{carb}}$ (Arthur et al., 1988; Arthur et al., 1985; Gröcke et al., 1999; Lini et al., 1992). In addition, some $\delta^{13}\text{C}_{\text{org}}$ curves are missing aspects of $\delta^{13}\text{C}_{\text{carb}}$ excursions due to depositional hiatuses. Despite this, these studies show the utility of $\delta^{13}\text{C}$ of terrestrial organic matter in illuminating changes in the carbon cycle.

The Rose Creek Pit, Southeastern Nebraska

The Rose Creek Pit (RCP) (Figs. 1A–B) is an inactive clay pit that exposes fluvial-estuarine deposits laid down on the eastern margin of the Western Interior Seaway (WIS) (Fig. 2) (Upchurch and Dilcher, 1990). The lower section consists of mudstone, interbedded with sandstones with abundant charcoal and vitrain along the margins in the lowest portion (below the first resistant sandstone; below ~1 m), with the Rose Creek leaf beds occurring between ~1–3 m (Figs. 1B and 3). The upper section is predominantly claystone, with a lignitic layer (5.3–5.55 m) containing abundant leaves, charcoal, and vitrain and abundant sphaerosiderites and pyrite in the paleosol (6.3–6.75 m) and above (Figs. 1B and 4). The sphaerosiderites and pyrite are indicative of wetland conditions due to a change in base-level caused to a eustatic lowering of sea levels at the ACB (Gröcke et al., 2006; Haq et al., 1987; Haq and Schutter, 2008; Ludvigson et al., 1998).

The Rose Creek Pit, Southeastern Nebraska

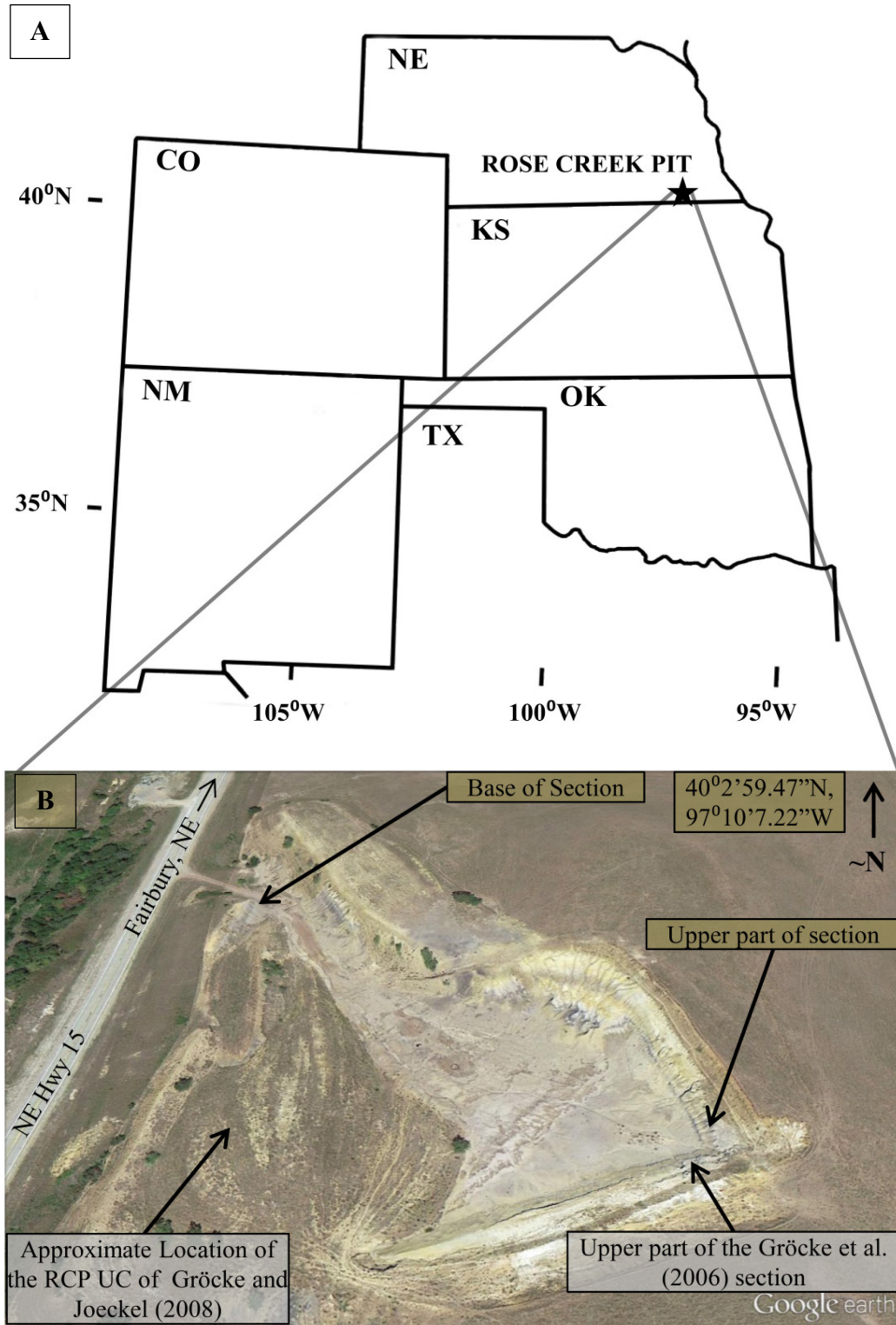


Figure 1: The Rose Creek Pit, Southeastern Nebraska. A) Map showing the location of the Rose Creek Pit. B) Google Earth (2013) satellite image of the RCP Locality, with locations of 2012 and 2013 sampling labeled. GPS coordinates were recorded at the center of RCP.

The Eastern Margin of the Western Interior Seaway, Middle Cretaceous

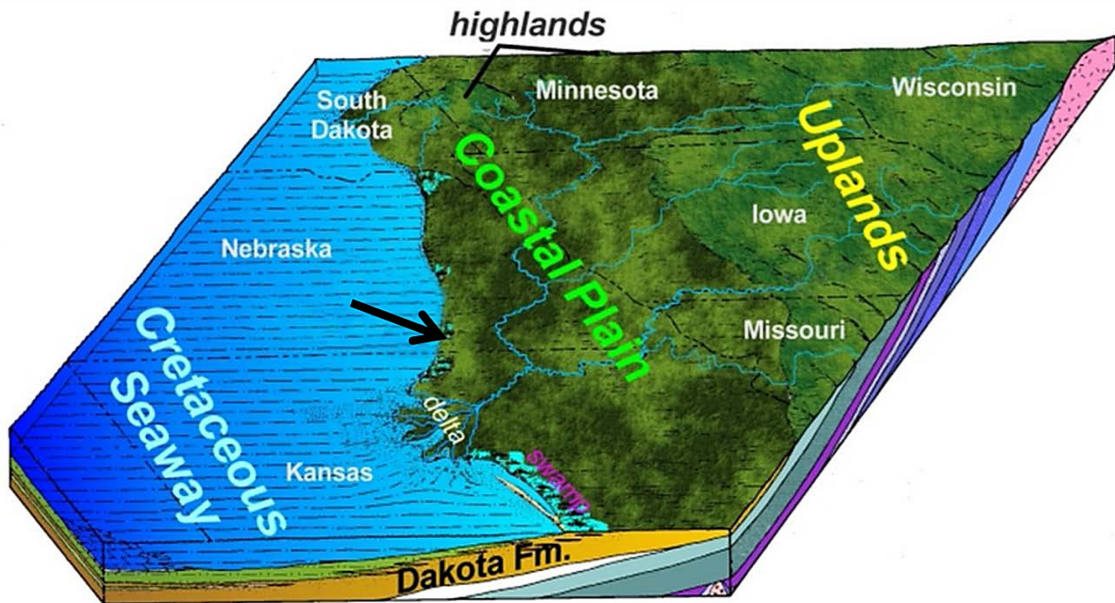
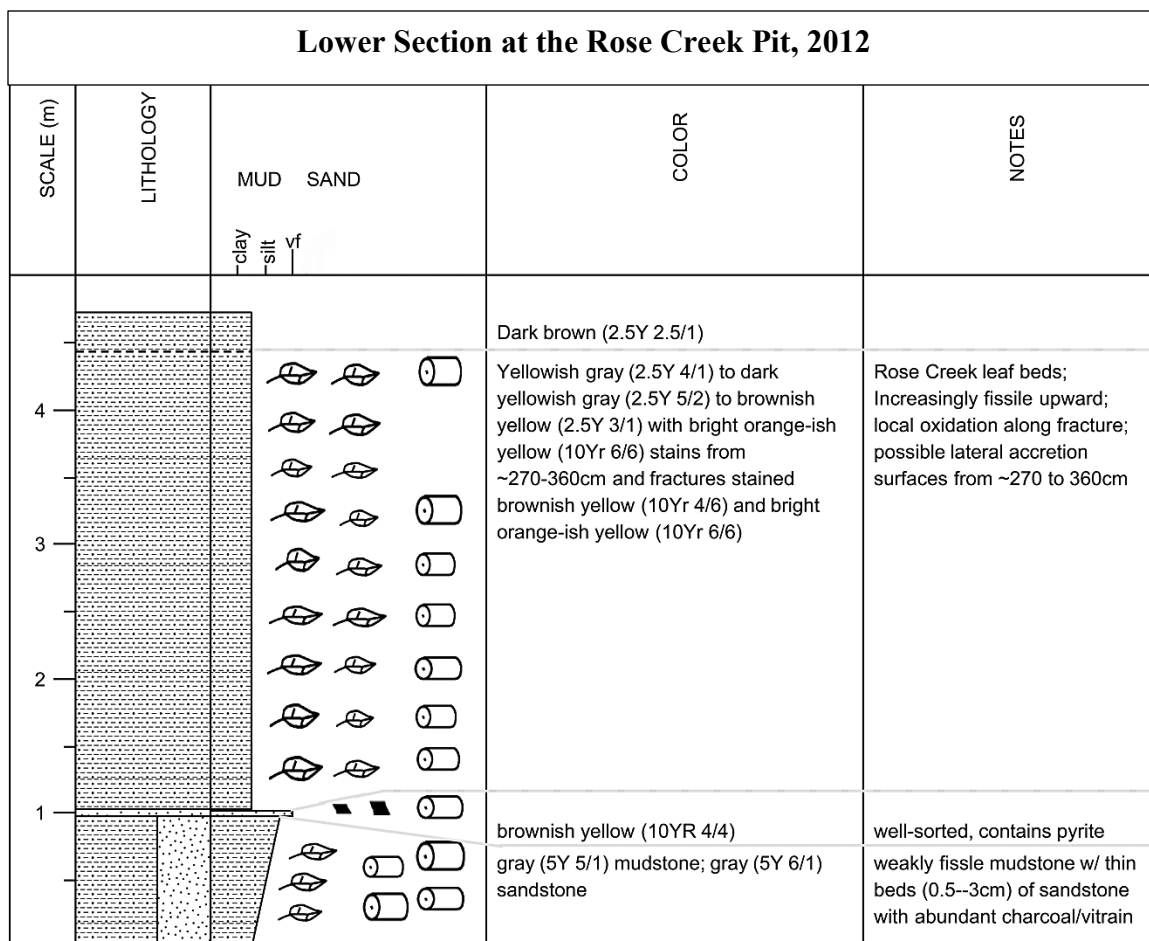


Figure 2: The Eastern Margin of the Western Interior Seaway, Middle Cretaceous. This figure presents the depositional environments that eventually formed the Dakota Formation and RCP locality. Image used by permission of Wikipedia contributor Anky-Man (2014), a vertebrate paleontologist, who redrew it from Hattin (1967).

The locality has been the site of palynological dating. Based on this analysis, RCP was originally dated as Cenomanian (Farley and Dilcher, 1986). Subsequent analysis by Robert Ravn found definitive Upper Albian palynomorphs (*Disaltriangulisporites perplexus* and *Podocarpidites multesimus*) low in the section and definitive Lower Cenomanian palynomorphs (*Foveogleicheniidites confossus* and *Artiopollis indivisus*) high in the section (Fig. 5) (Gröcke et al., 2006). This indicates that RCP preserves the ACB, the D₂ sequence boundary defined in Brenner et al. (2000), and OAE1d (Fig. 5) (Gröcke and Joeckel, 2008; Gröcke et al., 2006).

The Rose Creek Pit also preserves an abundant record of plant macrofossils and dispersed cuticle related to Lauraceae and other families (Figs. 3–4). Perhaps the best known plant fossil from RCP is the Rose Creek flower, which represents the oldest



 Mudstone

 Sandstone

 Claystone

 Lignite

 Leaf macrofossils/ dispersed cuticle

 Charcoal/vitrain

 Sphaerosiderite

 Pyrite

Figure 3: Lower Section at the Rose Creek Pit, 2012. The section was measured by Matt Joeckel, Greg Ludvigson, John Smith, Garland Upchurch, and Jon Richey in August 2012. From right to left, this figure features: 1) Measurement of the section in meters, starting at 0 m and ending at 4.5 m, 2) Lithology of the section, 3) Rough approximation of the location of plant fossils and minerals of note at RCP, 4) Description of the color of sediments within a lithological unit, 5) Features of lithological units.

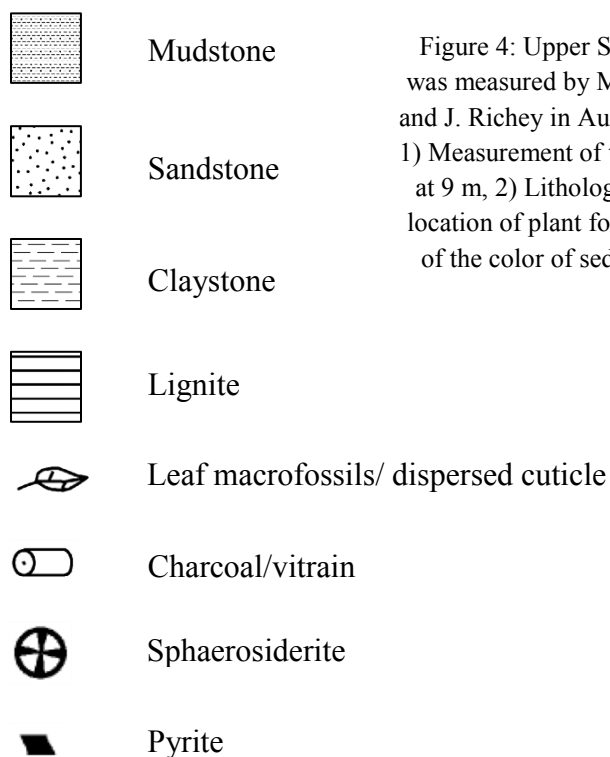
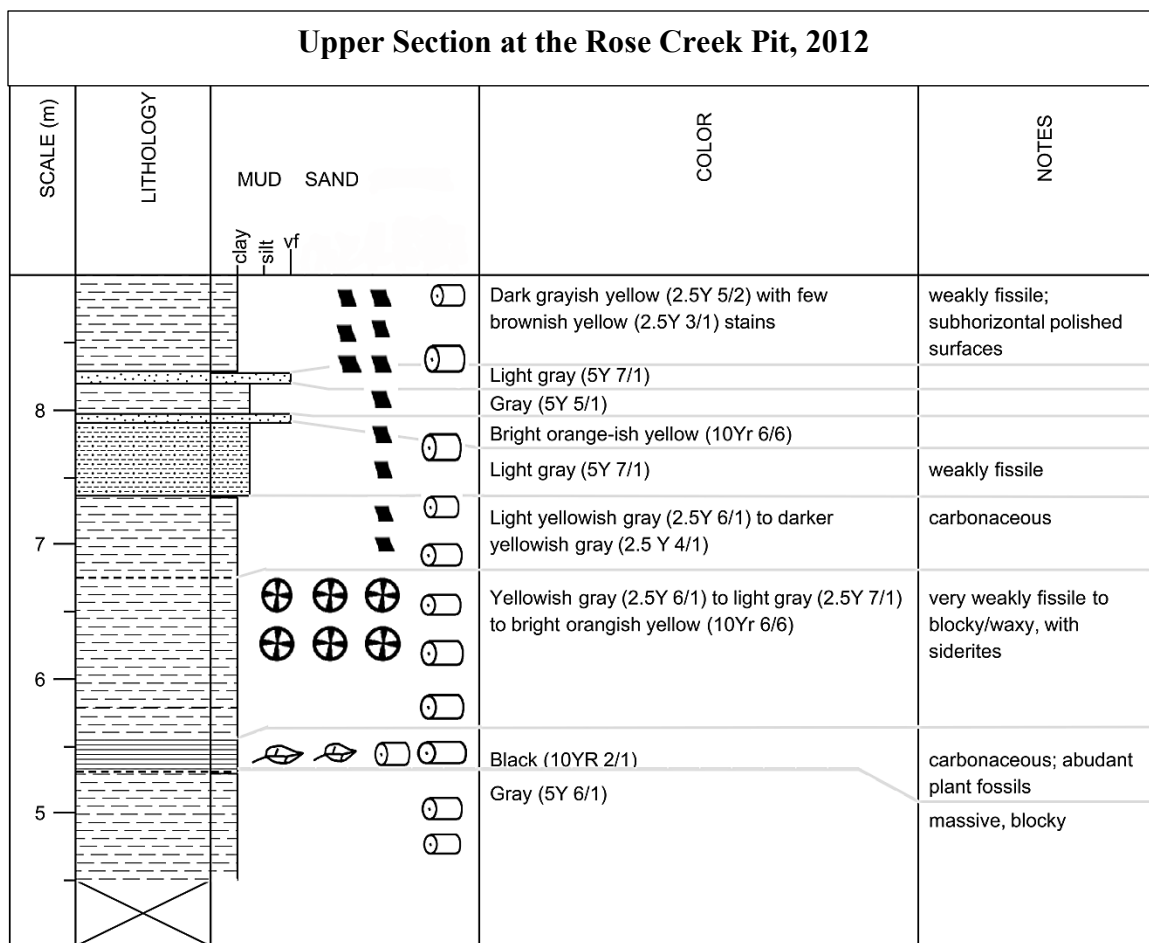


Figure 4: Upper Section at the Rose Creek Pit, 2012. The section was measured by M. Joeckel, G. Ludvigson, J. Smith, G. Upchurch, and J. Richey in August 2012. From right to left, this figure features: 1) Measurement of the section in meters, starting at 4.5 m and ending at 9 m, 2) Lithology of the section, 3) Rough approximation of the location of plant fossils and minerals of note at RCP, 4) Description of the color of sediments within a lithological unit, 5) Features of lithological units.

known eudicot flower of the clade Pentapetalae (Basinger and Dilcher, 1984; Cantino et al., 2007). The systematic affinities of the RCP leaf and cuticle flora is well established, because it is one of the few Cretaceous leaf macrofloras to be monographed using modern methods of foliar architecture and cuticular anatomy (Upchurch and Dilcher, 1990).

The Rose Creek locality also preserves charcoal and vitrain throughout the section and has been subject to detailed chemostratigraphic analysis (Figs. 3–4). Gröcke et al. (2006) produced $\delta^{13}\text{C}_{\text{char}}$ and $\delta^{13}\text{C}$ of bulk organics ($\delta^{13}\text{C}_{\text{bulk}}$) curves (Fig. 8B) that were correlated with a $\delta^{13}\text{C}$ curve of foraminifera ($\delta^{13}\text{C}_{\text{foram}}$, *Rotalipora* spp.) recovered at Ocean Drilling Project (ODP) site 1052 (Fig. 8G) (Wilson and Norris, 2001). The negative excursion found by Wilson and Norris (2001) during OAE1d was also seen in the $\delta^{13}\text{C}_{\text{char}}$ and $\delta^{13}\text{C}_{\text{bulk}}$, but the subsequent positive excursion was missing (Fig. 8A). This was interpreted as a ≈ 0.5 million year (Myr) depositional hiatus due to a global marine regressive event documented at the ACB (Gröcke et al., 2006). Gröcke and Joeckel (2008) later confirmed the reproducibility of the Gröcke et al. (2006) $\delta^{13}\text{C}_{\text{char}}$ and $\delta^{13}\text{C}_{\text{bulk}}$ curves with two additional $\delta^{13}\text{C}_{\text{bulk}}$ curves from sediment cores collected from within several meters of the RCP section face (Rose Creek Pit Upper Core [RCP UC]) and from ~ 2.6 km SSW of RCP (Core 13A05) (Fig. 8E). These core data were compared to the data of Gröcke et al. (2006) by aligning the beginning of the negative excursion. Both of these core $\delta^{13}\text{C}_{\text{bulk}}$ curves reproduced the negative excursion of Gröcke et al. (2006) and Wilson and Norris (2001) (Fig. 8E).

An important concern about the use of material collected at the RCP in $\delta^{13}\text{C}$ analysis is the possible marine influence at the locality. *Brachidontes* bivalves have been

recovered at RCP within the leaf beds, including one specimen in life position (Retallack and Dilcher, 1981). In addition, pyrite nodules are common, and there is evidence of rapid sediment deposition and polymodal crossbedding near RCP (Farley and Dilcher, 1986). This evidence suggests marine influence and higher-than-freshwater levels of salinity at RCP. This fits with the hypothesis of Hattin (1967) of extensive coastal swamps along the margins of the Western Interior Seaway during the Cretaceous. This poses a problem as salinity can have a significant effect on $\delta^{13}\text{C}_{\text{plant}}$ (Guy et al., 1980).

Evidence for this conclusion can be found at RCP. The leaf beds and dispersed cuticle of this locality are dominated by angiosperms (Upchurch and Dilcher, 1990). In fact, no gymnosperm cuticle has been observed in our section at RCP, despite the large amounts of cuticle isolated for this study. However, when I inspected fossil charcoal isolated at RCP, I found gymnosperm charcoal to be dominant, with some angiosperm charcoal present. These observations are consistent with facies analysis of Retallack and Dilcher (1981) and indicate that angiosperms grew in and around the depositional environment at RCP, while gymnosperms inhabited higher ground such as levees and the dry floodplains of the hinterland and were transported to RCP because charcoal floats, takes a great deal of time to waterlog, and has dispersal distances much greater than that of leaves. Therefore, for isotopic work at RCP, it is essential to perform the analysis on gymnosperm charcoal.

II. MATERIALS AND METHODS

On August 1–4, 2012, the RCP section was measured, and bulk sediment samples were collected at 30cm intervals throughout the ~9–10 m of exposed section at RCP by Jon Richey, Dr. Garland R. Upchurch, Dr. Matt Joeckel (University of Nebraska), Dr. Greg Ludvigson, and Dr. John Smith (Kansas Geological Survey) (Figs. 3–4). In addition, I made a second trip in 2013 to re-measure and verify the 2012 section (with the help of Dr. Matt Joeckel) and collected macro-charcoal samples where they occurred in the section in the manner of Gröcke et al. (2006). These samples were collected at the same interval as the collections of Gröcke et al. (2006), but the upper part of the section, in particular, was taken at a different position in the pit and shows significant differences to upper part of the Gröcke et al. (2006) section (Figs. 1, 3–5).

The lower part of the section was measured at the western end of the south wall of RCP, at approximately the same position of the lower part of the Gröcke et al. (2006) section (Figs. 1B and 5). However, the Gröcke et al. (2006) section began at the top of the resistant sandstone floor of the pit, while the section in this study began at the base of the vertical exposure, leading to a slight offset between the two sections (Fig. 5). For instance, a thin resistant sandstone layer, marking the bottom of the RCP leaf beds, is at ~1.1–1.2 m in the Gröcke et al. (2006) section (Fig. 5) and at ~1–1.04 m in the 2012 section, indicating an ~0.1 m offset. Also, the 2012 lower section was 4.5 m in height, while the Gröcke et al. (2006) lower section was 7 m (Fig. 5).

The upper section from Gröcke et al. (2006) was measured on the east end of the south wall of the pit (Figs. 1B and 5). However, this portion of the pit has undergone significant weathering in the 12 years between the measuring of the two sections

Comparison of the Lower and Upper Sections of This Study and the Lower and Upper Sections of Gröcke et al. (2006)

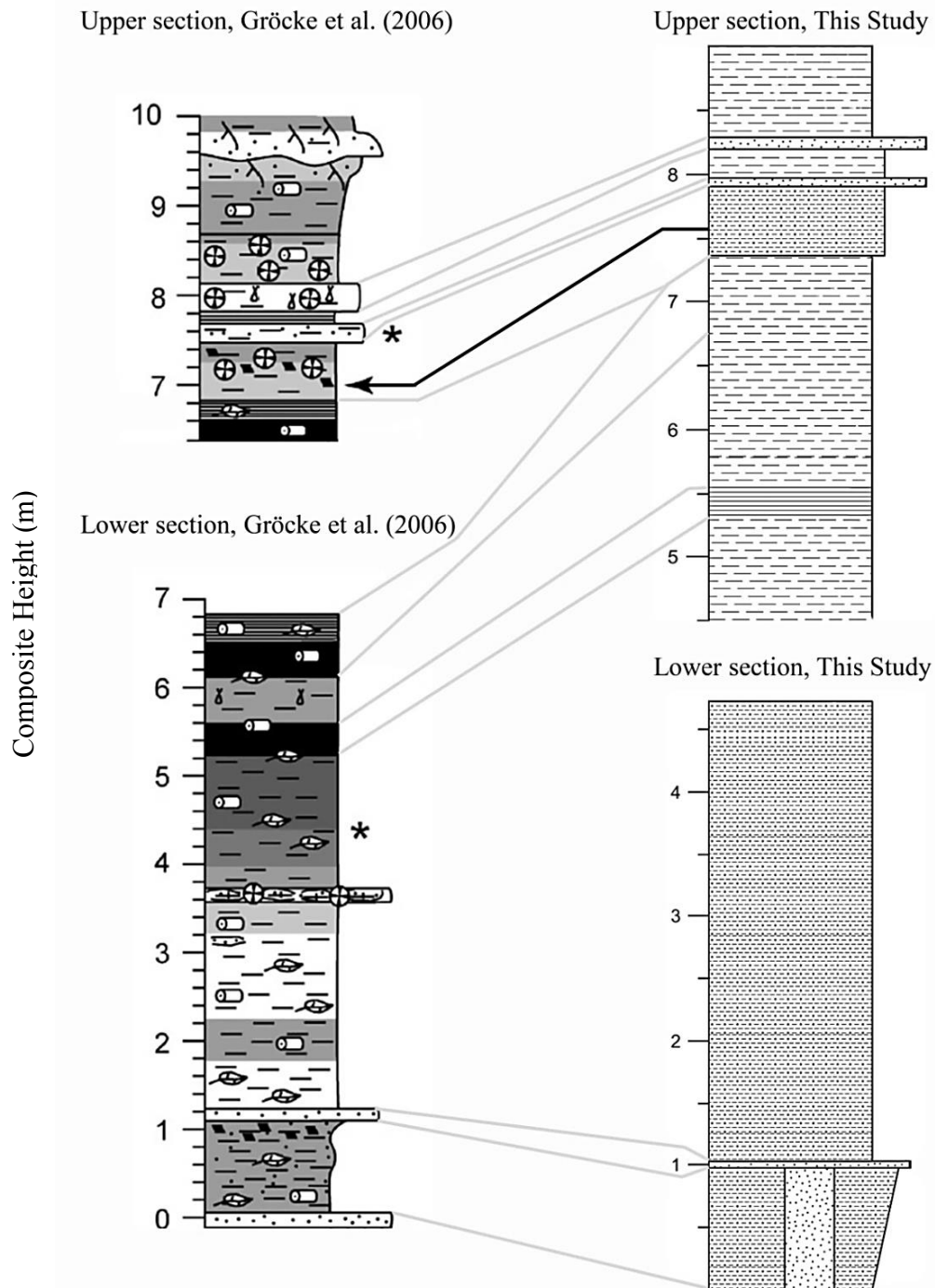


Figure 5: Comparison of the Lower and Upper Sections of This Study and the Lower and Upper Sections of Gröcke et al. (2006). The section of Gröcke et al. (2006) was measured by Stuart Robinson, Darren Gröcke, G. Ludvigson, and M. Joeckel in October 2002. The gray lines connect resistant sandstones and carbonaceous beds and the black line connects the ACB in Gröcke et al. (2006) to the approximate location of the ACB in the section from this study (Note: the upper lignite in Gröcke et al. (2006) section corresponds to a carbonaceous mudstone in my section). The stars show the location of palynological analysis by Gröcke et al. (2006).

(collections for Gröcke et al. (2006) took place in 2002) and a large gully has formed near where the Gröcke et al. (2006) upper section was measured. Due to this, the 2012 upper section was measured 3–4 m north, on the east end of the north wall of the pit (i.e. on the opposite side of the gully) (Fig. 1B). The upper section of the RCP features two carbonaceous layers. In the Gröcke et al. (2006) section, there are lignites at ~5.2–5.6 m and ~6.1–7.6 m, respectively. In the 2012 section, there is a lignite at 5.3–5.55 m that corresponds to the lower lignite in Gröcke et al. (2006). However, in my section the second carbonaceous layer (6.75–7.35 m) was found to be carbonaceous claystone (Fig. 5). This discrepancy is most likely due to lateral variation in facies. In addition, the upper part of RCP contains 2 thin layers of very fine sandstone. In the Gröcke et al. (2006) section, they are found at ~7.5–7.65 m and 7.8–8.15 m. In the 2012 section, they are at 7.9–7.97 m and 8.2–8.28 m (fig. 5). This is most likely due to lateral variation in the thickness of individual lithologies, as both the thicknesses of those listed above and the sediment that separate them vary. During the return trip I made to RCP in 2013, I attempted to reconcile the differences in the 2012 section and the section of Gröcke et al. (2006). I verified that the 2012 section was accurate and the sections of Gröcke et al. (2006) and this study are similar enough to make comparisons of the individual geochemistry curves (Fig. 5). In summary, the discrepancies between the Gröcke et al. (2006) section and my section probably result from: 1) the difference in height of the two component sections, and 2) the difference in location of the two upper sections.

Gröcke and Joeckel (2008) later generated two additional $\delta^{13}\text{C}_{\text{bulk}}$ curves from sediment cores collected by the University of Nebraska-Lincoln Conservation and Survey Division in 2004 within several meters of the RCP section face (Rose Creek Pit Upper

Core [RCP UC], Fig. 1B) and ~2.6 km SSW of RCP (Core 13A05). These core data were compared to those of Gröcke et al. (2006) by aligning the beginning of the negative excursion and will be compared to this study by the same means.

For this study, bulk sediment samples were collected at ~0.3 m intervals throughout the 9 m pit face at RCP. Bulk sediment samples were restricted to the width of the chisel edge rock hammer (~2.5 cm) to minimize time-averaging. In addition to those samples, samples were collected without the 2.5 cm restriction when larger samples were needed to isolate sufficient amounts of cuticle and charcoal for analysis. For each sample, ~300–1000 g of sediment were disaggregated by soaking in 10% hydrochloric acid (HCl) overnight, repeated rinsing until neutral, and treatment by a saturated solution of sodium pyrophosphate with a few milliliters of 30% hydrogen peroxide added. Cuticle, charcoal, and vitrain were isolated and separated using 90 and 500 μm sieves. Dispersed cuticle was macerated in various combinations of 10% chromium trioxide, household bleach, and/or sodium pyrophosphate, and mounted in glycerin jelly. Cuticle was observed with a Zeiss Photoscope I microscope using brightfield optics and photographed with a Cannon Eos Digital Rebel XSi camera (12-megapixel resolution) at 200x magnification. In cases where cuticle was highly folded and/or degraded, image stacks were made using CombineZP[©] and were manipulated to improve contrast using Adobe Photoshop[®] CS6 (Adobe[®], 2012; Hadley, 2010). ImageJ[©] was used to count epidermal cells and stomata for calculating SI (Rasband, 1997). The target species was *Pandemophyllum kvacekii* (Fig. 6A), but morphotypes were established for all lauraceous cuticles (Figs. 7A and 7B) and these morphotypes were counted. *Pabiania variloba* (Fig. 6B), whose systematic affinities are with Lauraceae, Hernandiaceae, and related families

Species Used in Stomatal Index Analysis.

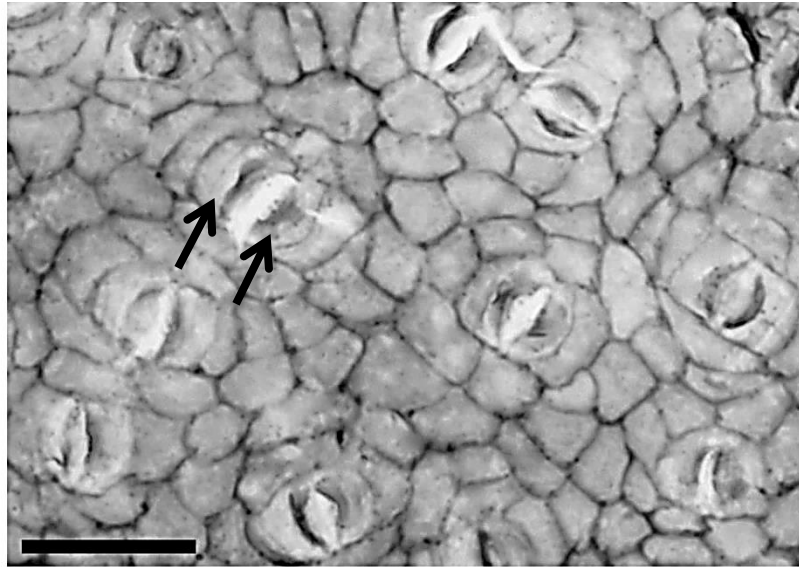


Figure 6A: Species Used in Stomatal Index analysis. Cuticle of *P. kvacekii* collected at RCP (125x, scale = 50 μ m). This cuticle features brachyparacytic to hemiamphibrachyparacytic to amphibrachyparacytic stomata, spindle-shaped embedded guard cells, and scale-shaped thickenings that do not extend to the full length of the guard cells. The scale shaped thickenings are generally best developed where the inner subsidiary cells meet the guard cells. Stomatal complexes of *P. kvacekii* also have embedded subsidiary cells below the inner pair of subsidiary cells (black arrows). Some specimens also have trichome bases with heavily cutinized angular to round pores and radially aligned surrounding cells.

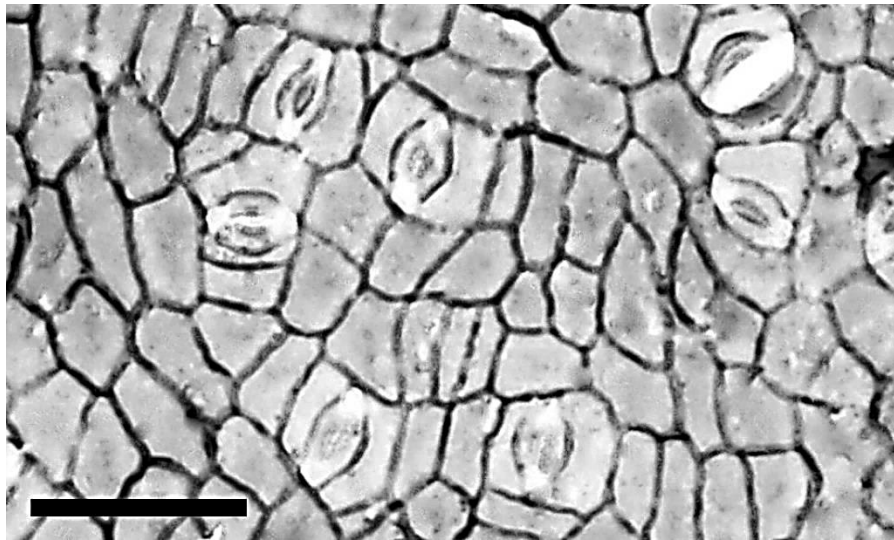


Figure 6B: Species Used in Stomatal Index analysis. Cuticle of *P. variloba* collected at RCP (125x, scale = 50 μ m). This cuticle features brachyparacytic stomata, but also has rare laterocytic, hemiparacytic, and cyclocytic stoma. Some specimens have lamellar shaped thickenings that do not extend the full length of the guard cells, others are missing this feature. Trichome bases are rarely present. Specimens with trichome bases have heavily-cutinized pores and some associated cells.

Pandemophyllum Morphotypes Used in Stomatal Index Analysis.

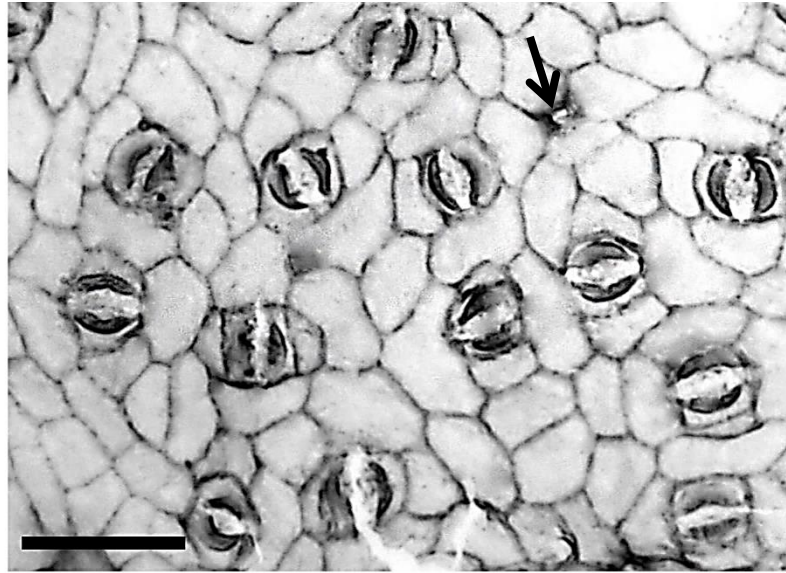


Figure 7A: *Pandemophyllum* Morphotypes Used in Stomatal Index Analysis. Cuticle of Morphotype 5 collected at RCP (125x, scale = 50 μ m). This cuticle features brachyparacytic to hemiamphibrachyparacytic to amphibrachyparacytic stomata, spindle-shaped embedded guard cells, and scale-shaped thickening that mostly do not extend to the full length of the guard cells. This species also has common trichome bases with heavily cutinized angular to round pores and radially aligned surrounding cells in most bases (black arrow). These features are identical to *P. kvacekii*. However, Morphotype 5 has much thicker lamellar-shaped thickenings that are thickest on the inner and outer edges.

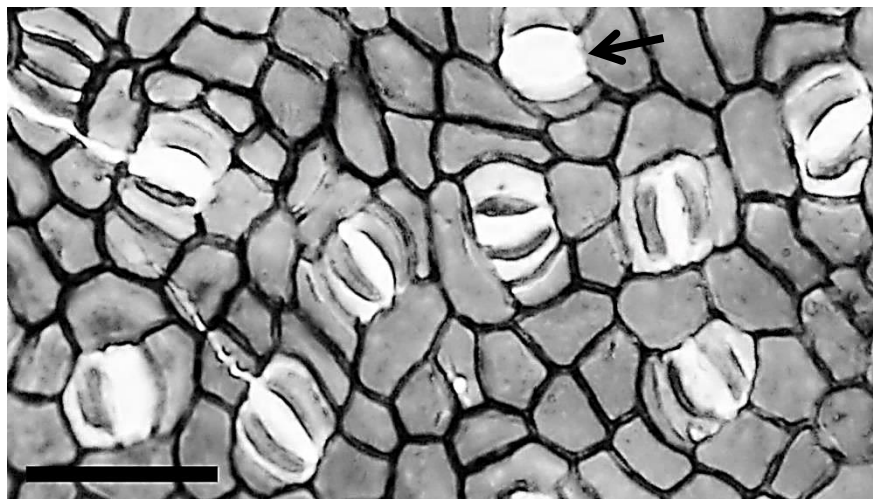


Figure 7B: *Pandemophyllum* Morphotypes Used in Stomatal Index Analysis. Cuticle of Morphotype 8 collected at RCP (125x, scale = 50 μ m). This cuticle shared all the features listed for *P. kvacekii* and Morphotype 5. It has lamellar-shaped thickenings similar to Morphotype 5. The most notable difference between Morphotype 5 and the other *Pandemophyllum* species/morphotypes is that no trichome bases were observed in this species and that the guard cells and inner subsidiary cells are often missing ("stomatal punchouts"[Upchurch, Pers. Comm.], black arrow).

of Laurales, was abundant throughout the section and also was counted (Upchurch and Dilcher, 1990). Overall SI was calculated by taking the average of all lauraceous cuticles counted in each sampling interval, excluding *P. variloba*. In addition, SI (Eq. 2) was calculated for each morphotypes and *P. variloba*. This allowed me to determine the extent to which taxonomy influenced my results given that SI is species specific. A total of 5000 cells were counted in each individual cuticle, when possible, because this is the number of cells where variation in SI was decreased. A total of 172,812 epidermal cells were counted among all samples.

Transfer functions derived from modern and fossil lauraceous species were used to estimate CO₂ levels from SI calculated in this study (Barclay et al., 2010; Kürschner et al., 2008). Kürschner et al. (2008) derived an equation to predict Miocene CO₂ using the fossil lauraceous species *Laurophyllum pseudoprinceps* (Eq. 4). To do this, Kürschner et al. (2008) first calculated stomatal response curves from the modern species *Laurus nobilis* and *Ocotea foetens* using herbarium specimens and historic CO₂ concentrations. They then cross-calibrated *Laurophyllum pseudoprinceps* with these two extant species of Lauraceae and *Ginkgo biloba* in strata where they co-occur. The *L. pseudoprinceps* equation is,

$$\text{CO}_2 = -46.011 * \text{SI}_f + 993.37 \quad [4],$$

where SI_f = SI from fossil lauraceous cuticle. In order to assess the range of possible CO₂ values using the Kürschner et al. (2008) transfer function, the standard deviation (SD) of the average *Pandemophyllum* SI was calculated when possible and SI ± one SD was inserted into the equation above.

Barclay et al. (2010) used herbarium specimens of *Hypodaphnis zenkeri* and the *L. nobilis* data of Kürschner et al. (2008) to create two new transfer functions to predict CO₂ during OAE2 using fossil lauraceous cuticle (Eq 5–6). This resulted in the following relationship for *L. nobilis*,

$$\text{CO}_2 = (-168.39 * \text{Ln}[\text{SI}_f]) + 790.93 \quad [5],$$

and this relationship for *H. zenkeri*,

$$\text{CO}_2 = (-27.447 * \text{SI}_f) + 559.67 \quad [6].$$

Barclay et al. (2010) also derived separate \pm 95% confidence interval (CI) equations to estimate the error in the statistical relationship between SI and CO₂ for modern species (Eq 7–10). For *L. nobilis* they are,

$$-95\% \text{ CI} = (-9.3347 * \text{SI}_f) + 467.28 \quad [7]$$

$$+95\% \text{ CI} = (0.9177 * [\text{SI}_f]^2) - (42.578 * \text{SI}_f) + 777.21 \quad [8],$$

and for *H. zenkeri* they are,

$$-95\% \text{ CI} = (-10.279 * [\text{SI}_f]^2) + (132.43 * \text{SI}_f) - 64.375 \quad [9]$$

$$+95\% \text{ CI} = (19.634 * [\text{SI}_f]^2) + (401.15 * \text{SI}_f) + 2341.8 \quad [10].$$

Carbon isotope values were measured using fossil gymnosperm charcoal ($\delta^{13}\text{C}_{\text{gym}}$) and vitrain ($\delta^{13}\text{C}_{\text{vit}}$). Charcoal and vitrain were separated from cuticle and other organics by swirling each sample in H₂O and pouring off the cuticle until only charcoal and vitrain remained. Charcoal in each sample was inspected under a stereomicroscope, and angiosperm charcoal was separated from gymnosperm charcoal. This was not possible with vitrain isolated at RCP, because vitrain does not preserve anatomy. Angiosperm charcoal was not used to construct the isotopic curve. This is because, at certain levels in the section, the $\delta^{13}\text{C}$ of angiosperm charcoal was 2–3‰ more negative

than the $\delta^{13}\text{C}$ of gymnosperm charcoal, while at other levels there was no difference. The lower $\delta^{13}\text{C}$ of angiosperms at certain stratigraphic levels most likely reflects greater hydraulic conductance, which increases stomatal conductance and p_i/p_a (Eq. 3), and therefore, lowers $\delta^{13}\text{C}$ and Water Use Efficiency (WUE) (McCarroll and Loader, 2004).

As reviewed earlier, many factors (irradiance, nutrient availability, water stress, salinity, taxonomy, etc.) affect the $\delta^{13}\text{C}$ signal from plants. In this study, salinity is a particular concern due to the marine influence at the RCP locality. To minimize the effect of these environmental factors on $\delta^{13}\text{C}$, charcoal and vitrain samples were sorted according to size, and the smallest fraction was homogenized for analysis. This was done because it has been suggested that homogenized organic matter from a sufficiently large area represents a regional $\delta^{13}\text{C}$ signal, which dampens local environmental effects (Ando and Kakegawa, 2007; Hasegawa, 2003).

Charcoal and vitrain samples were placed in 3M HCl to remove any carbonates present, and heated to 60°C to remove pyritic compounds. Isotope values were calculated using a Costech Elemental Analyzer[®] located in the lab of Dr. Marina Suarez at the University of Texas at San Antonio. This machine works by combusting material at 1000°C, to produce CO₂ gas, which is then analyzed via continuous-flow isotope ratio mass spectrometry on a ThermoFinnigan Delta + XP. Carbon isotope values are measured vs. internal working gas and calibrated using international standards with external precision of $\pm 0.06\text{‰}$.

III. RESULTS

Geochemistry

Carbon isotope values ($\delta^{13}\text{C}_{\text{char}}$ and $\delta^{13}\text{C}_{\text{bulk}}$) from across Hwy. 15 from RCP indicate that pre-excursion values were ~ -23 to -23.7‰ (avg. = -23.38‰) (Fig. 8B) (Gröcke et al., 2006). In this study, at 0 m in the RCP section (i.e. immediately above the resistant sandstone floor), $\delta^{13}\text{C}_{\text{gym}}$ begins at -25.15‰ and $\delta^{13}\text{C}_{\text{vit}}$ begins at -24.74‰ (Fig. 8C). Between 0.9 m and 1.2 m, both curves are most negative, with a depletion of 1.2‰ in $\delta^{13}\text{C}_{\text{gym}}$ and 1.47‰ in $\delta^{13}\text{C}_{\text{vit}}$ compared to the samples at 0 m, and a depletion of 2.96‰ in $\delta^{13}\text{C}_{\text{gym}}$ and 2.83‰ in $\delta^{13}\text{C}_{\text{vit}}$ compared to the Gröcke et al. (2006) pre-excursion samples (Fig. 8D). In both curves, the negative $\delta^{13}\text{C}$ excursion ends (i.e. the last negative value before $\delta^{13}\text{C}$ returns to \sim pre-excursion values) at ~ 3.3 – 3.6 m. Vitrain $\delta^{13}\text{C}$ values hover at or slightly above pre-excursion values through the rest of the section. However, in the $\delta^{13}\text{C}_{\text{gym}}$ curve, there is a slight positive excursion, with samples more positive than pre-excursion values at 4.5 m ($+0.56\text{‰}$), 5.1 m ($+2.27\text{‰}$), and 5.4 m ($+0.92\text{‰}$), with values at or above pre-excursion values between those samples (Fig. 8C). From this slight positive enrichment, $\delta^{13}\text{C}_{\text{gym}}$ hovers at or around pre-excursion values throughout the final 3.5 m of section.

The $\delta^{13}\text{C}_{\text{gym}}$ and $\delta^{13}\text{C}_{\text{vit}}$ curves are remarkably similar during many portions of the section at RCP. Values at 0–0.3 m are closely grouped (-24.74 to -25.55‰) and both curves are most negative at 0.9–1.2 m (Fig. 8C). In addition, the duration of the negative excursions are similar in length and both show a slight enrichment in values during th

Chemostratigraphy of the Rose Creek Pit Area, Compared to Wilson and Norris (2001)

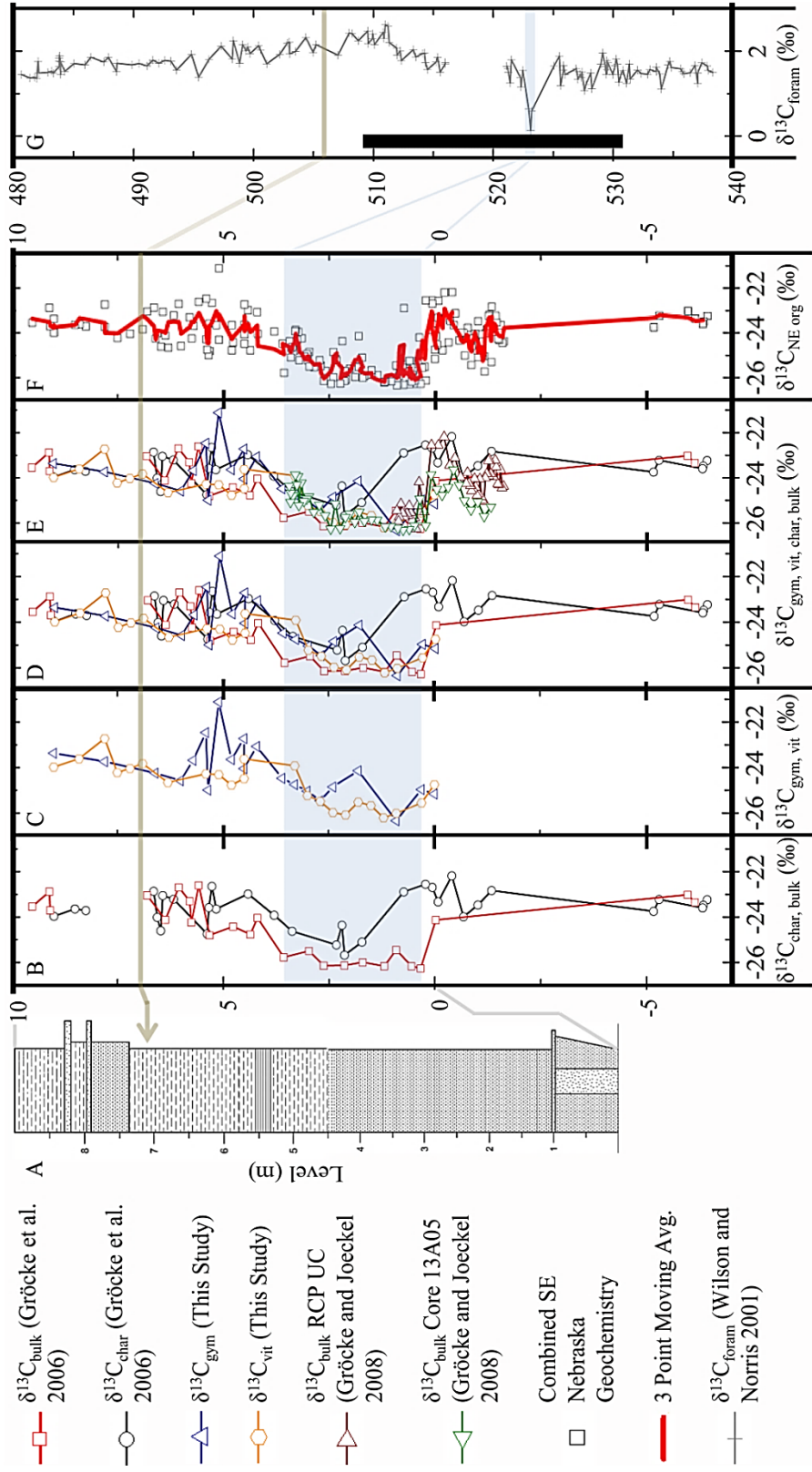


Figure 8. Chemostratigraphy of the Rose Creek Pit Area, Compared to Wilson and Norris (2001). The brown line is the ACB. The blue box marks the negative excursion. A) The RCP section from this study. B) $\delta^{13}\text{C}_{\text{char}}$ (red squares) and $\delta^{13}\text{C}_{\text{bulk}}$ (black circles) from RCP and across NE Hwy 15 (Gröcke et al., 2006). C) $\delta^{13}\text{C}_{\text{gym}}$ (blue triangles) and $\delta^{13}\text{C}_{\text{vit}}$ (orange hexagons) from RCP. D) Data from fig. 3B and 3C combined. E) Data from fig. 3B and 3C combined with $\delta^{13}\text{C}_{\text{bulk}}$ from cores drilled close to RCP (RCP UC, maroon right-facing triangles and Core 13A05, green left-facing triangles) (Gröcke and Joeckel, 2008). F) Scatterplot of all Southeastern Nebraska geochemistry (black boxes). Red line is a 3-pt. moving average. (Gröcke and Joeckel, 2008; Gröcke et al., 2006). G) $\delta^{13}\text{C}_{\text{foram}}$ (*Rotailipora* spp.) isolated from ODP Site 1052. Blake Nose, western Atlantic. The black bar indicates occurrence of black shale (Wilson and Norris, 2001).

overall negative excursion at 1.8 m. Also, values between 6.6–9 m are very similar and show the same general trend. The largest difference between the sections is the slight enrichment in $\delta^{13}\text{C}_{\text{gym}}$ from 4.5–5.4 m.

As stated earlier, $\delta^{13}\text{C}_{\text{char}}$ and $\delta^{13}\text{C}_{\text{bulk}}$ samples from across Hwy. 15 from RCP indicate that pre-excursion values were ~ -23 to -23.7‰ (Gröcke et al., 2006) (Fig. 8B). Gröcke et al. (2006) collected charcoal below the resistant sandstone floor at RCP. Charcoal $\delta^{13}\text{C}$ values from this interval shows an enrichment ($\sim +1.5\text{‰}$) before the negative excursion begins. Bulk samples began at the floor of RCO and, therefore, $\delta^{13}\text{C}_{\text{bulk}}$ does not capture this enrichment (Fig. 3). At the end of the slight enrichment in the $\delta^{13}\text{C}_{\text{char}}$ curve, and at the level of the sandstone on the floor of RCP or slightly above, $\delta^{13}\text{C}_{\text{bulk}}$ undergoes a rapid negative excursion, going from -24.14‰ to its most negative value -26.28‰ at ~ 0.44 m (Fig. 8B). Charcoal $\delta^{13}\text{C}$ values also shows a negative excursion of $\sim 2.31\text{‰}$, but the onset of the negative excursion is delayed relative to the $\delta^{13}\text{C}_{\text{bulk}}$ curve and the $\delta^{13}\text{C}_{\text{gym}}$ and $\delta^{13}\text{C}_{\text{vit}}$ curves. However, this appears to be a relative lack of data during the negative excursion, as the delayed shift is due to a single data point at 0.9 m, which is $\sim 2.5\text{--}3\text{‰}$ higher than any data point. Gröcke and Joeckel (2008) suggested the possibility that that particular sample could be reworked from older sediments and not representative of the true $\delta^{13}\text{C}$ during that interval. In the Gröcke et al. (2006) $\delta^{13}\text{C}_{\text{char}}$ curve, the most negative value is found at 2.2 m (Fig. 5B).

The duration of the negative excursion in the $\delta^{13}\text{C}_{\text{char}}$ and $\delta^{13}\text{C}_{\text{bulk}}$ in the Gröcke et al. (2006) study is ~ 3.64 m and ~ 3.88 m, respectively, a duration similar to that of $\delta^{13}\text{C}_{\text{gym}}$ and $\delta^{13}\text{C}_{\text{vit}}$ in of this study (3.3–3.6 m) (Fig. 8D). From that level, $\delta^{13}\text{C}_{\text{char}}$ and $\delta^{13}\text{C}_{\text{bulk}}$ values hover at or slightly above pre-excursion values, similar to the $\delta^{13}\text{C}_{\text{gym}}$ and

$\delta^{13}\text{C}_{\text{vit}}$ curves of this study with a few exceptions. However, there are a few discrepancies between our curves (Fig. 5). First, Gröcke et al. (2006) found or collected no bulk organic matter or charcoal between 6.6–8.6 m due to a paleosol in that interval, which they hypothesized was due to a ~ 0.5 Myr depositional hiatus caused by a regressive event at the ACB (Fig. 8B and D). They further hypothesized that the absence of the positive phase of the excursion at RCP indicated a depositional hiatus in the interval of the paleosol (Gröcke et al., 2006). Second, several $\delta^{13}\text{C}_{\text{char}}$ and $\delta^{13}\text{C}_{\text{bulk}}$ values high up in the section were enriched relative to pre-excursion values. In the $\delta^{13}\text{C}_{\text{char}}$ curve, those enriched values were found at 4.41 m (+0.41‰), 5.27 m (+0.74‰), and 6.64m (+0.53‰), and in the $\delta^{13}\text{C}_{\text{bulk}}$ curve, they were found at 5.58 m (+0.78‰) and 6.05m (+0.69‰). The interval in which the enriched values appear in the Gröcke et al. (2006) $\delta^{13}\text{C}_{\text{char}}$ and $\delta^{13}\text{C}_{\text{bulk}}$ curves (4.41–6.64 m) overlaps the interval where enriched values occurs in the $\delta^{13}\text{C}_{\text{gym}}$ and $\delta^{13}\text{C}_{\text{vit}}$ curves (4.5–5.4 m) (Figs. 8B and D).

The RCP UC and Core 13A05 $\delta^{13}\text{C}_{\text{bulk}}$ curves from Gröcke and Joeckel (2008) also show a high level of similarity to the $\delta^{13}\text{C}_{\text{gym}}$, $\delta^{13}\text{C}_{\text{vit}}$, $\delta^{13}\text{C}_{\text{char}}$, and $\delta^{13}\text{C}_{\text{bulk}}$ curves of this study and Gröcke et al. (2006), despite being collected in different locations and being compared to the other curves by aligning the negative excursion (Fig. 8E). During the lowest part of the two core $\delta^{13}\text{C}_{\text{bulk}}$ curves, there is a distinct offset in average $\delta^{13}\text{C}$ values of $\sim 1\%$, which was attributed to possible differing organic inputs and/or preservation between the two cores (Gröcke and Joeckel, 2008). Despite this, both core curves show the enrichment seen in the $\delta^{13}\text{C}_{\text{char}}$ curve of Gröcke et al. (2006). The enrichment is $\sim 1.4\%$ for the RCP UC core and $\sim 1\%$ for Core 13A05, similar to the enrichment in the $\delta^{13}\text{C}_{\text{char}}$ curve of Gröcke et al. (2006) ($\sim 1.5\%$) (Fig. 8E). Following

this enrichment, both core curves show rapid negative excursions. For the Core 13A05 $\delta^{13}\text{C}_{\text{bulk}}$ curve, the magnitude of the negative excursion is $\sim 2.4\%$, while the RCP UC $\delta^{13}\text{C}_{\text{bulk}}$ curve shows a negative excursion of $\sim 2.0\%$. This is similar to the magnitude of the negative excursions in the other $\delta^{13}\text{C}$ curves ($2.14\text{--}2.96\%$) (Fig. 8E). For the Core 13A05 $\delta^{13}\text{C}_{\text{bulk}}$ curve, the duration of the negative excursion (~ 3 m) is similar to the duration of the negative excursion in the other curves ($3.3\text{--}3.88$ m). However, the duration of the negative excursion for the RCP UC $\delta^{13}\text{C}_{\text{bulk}}$ curve is not known, as that curve does not contain a return to pre-excursion value, meaning it does not capture the full negative excursion (Fig. 8E).

When the $\delta^{13}\text{C}_{\text{gym}}$, $\delta^{13}\text{C}_{\text{vit}}$, $\delta^{13}\text{C}_{\text{char}}$, and $\delta^{13}\text{C}_{\text{bulk}}$ data of this study, Gröcke et al. (2006), and Gröcke and Joeckel (2008) are plotted as a scatterplot with a 3-point moving average, the trends discussed above are clear (Fig. 8F). The pre-excursion values from samples collected across Hwy. 15 from RCP hover around $\sim -23.4\%$. From there, there appears to be a slight negative shift, but this is an artifact of the offset between the absolute $\delta^{13}\text{C}$ values from RCP UC and Core 13A05. Despite this, the enrichment before the negative is captured in the 3-point moving average, though the magnitude to the enrichment is dampened because of the offset between values from the two cores (Fig. 5F). Following the enrichment, the rapid negative excursion occurs, with the 3-point moving average moving from $\sim -23\%$ at ~ 0.1 m to $\sim -26.1\%$ at ~ 0.46 m. The duration of the negative excursion is ~ 3.3 m (Fig. 8F). From there, the curve hovers at or slightly above pre-excursion values throughout the negative excursion. The slight enrichment seen in some $\delta^{13}\text{C}_{\text{gym}}$, $\delta^{13}\text{C}_{\text{char}}$, and $\delta^{13}\text{C}_{\text{bulk}}$ data points of this study and Gröcke et al. (2006) from $4.41\text{--}6.64$ m is not evident in the 3-point moving because there are only

eight enriched data points interspersed among many data points in the interval that are at or slightly more negative than pre-excursion values (Fig. 8F).

Gröcke et al. (2006) related the negative excursion in their $\delta^{13}\text{C}_{\text{char}}$ and $\delta^{13}\text{C}_{\text{bulk}}$ curves to the $\delta^{13}\text{C}_{\text{foram}}$ curve (*Rotalipora* spp. isolated from ODP Site 1052, Blake Nose, western Atlantic) of Wilson and Norris (2001) (Fig. 8G). The sedimentary duration of the negative excursion in SE Nebraska (avg. $\approx 2.21\text{‰}$ over ~ 3.3 m of section) corresponds to a $\sim 1.4\text{‰}$ negative excursion in $\delta^{13}\text{C}_{\text{foram}}$, spanning ~ 1 m of pelagic marine sediment.

Stomatal Index and CO₂

At the beginning of the negative excursion, average SI for *Pandemophyllum* is ~ 8.2 (Fig. 9C). Among all $\delta^{13}\text{C}$ curves, the sedimentary duration of the negative excursion is ~ 3.3 m, with the exception of the RCP core, where it is impossible to know if the full negative excursion has been sampled (Figs. 9A and B). Stomatal Index changes during the negative excursion in $\delta^{13}\text{C}$ with a gradual decrease from ~ 8.2 to 5.1, though this trend is not constant (Fig. 9C). After the initial drop in SI from 8.2 to 6.15, SI suddenly rises back to 8.3 at ~ 1.2 m, then continues its descent, with another small rise in values ~ 1.8 m. The duration of this gradual decrease in SI is the same as the duration of the negative isotopic excursion (~ 3.3 m). Average SI tracks the return to pre-excursion values by rising to ~ 7.97 . Following this, there is an interval where no cuticle samples were recovered (4.5–5.35 m). At 5.35 m (the lignite layer), average SI drops to 7.57. No cuticle samples were recovered above 5.35 m at RCP, despite processing large quantities of sample (Fig. 9C). The gradual decrease in SI during the negative $\delta^{13}\text{C}$ excursion, as

Carbon Isotopes and Stomatal Index from Rose Creek Pit, Southeastern Nebraska

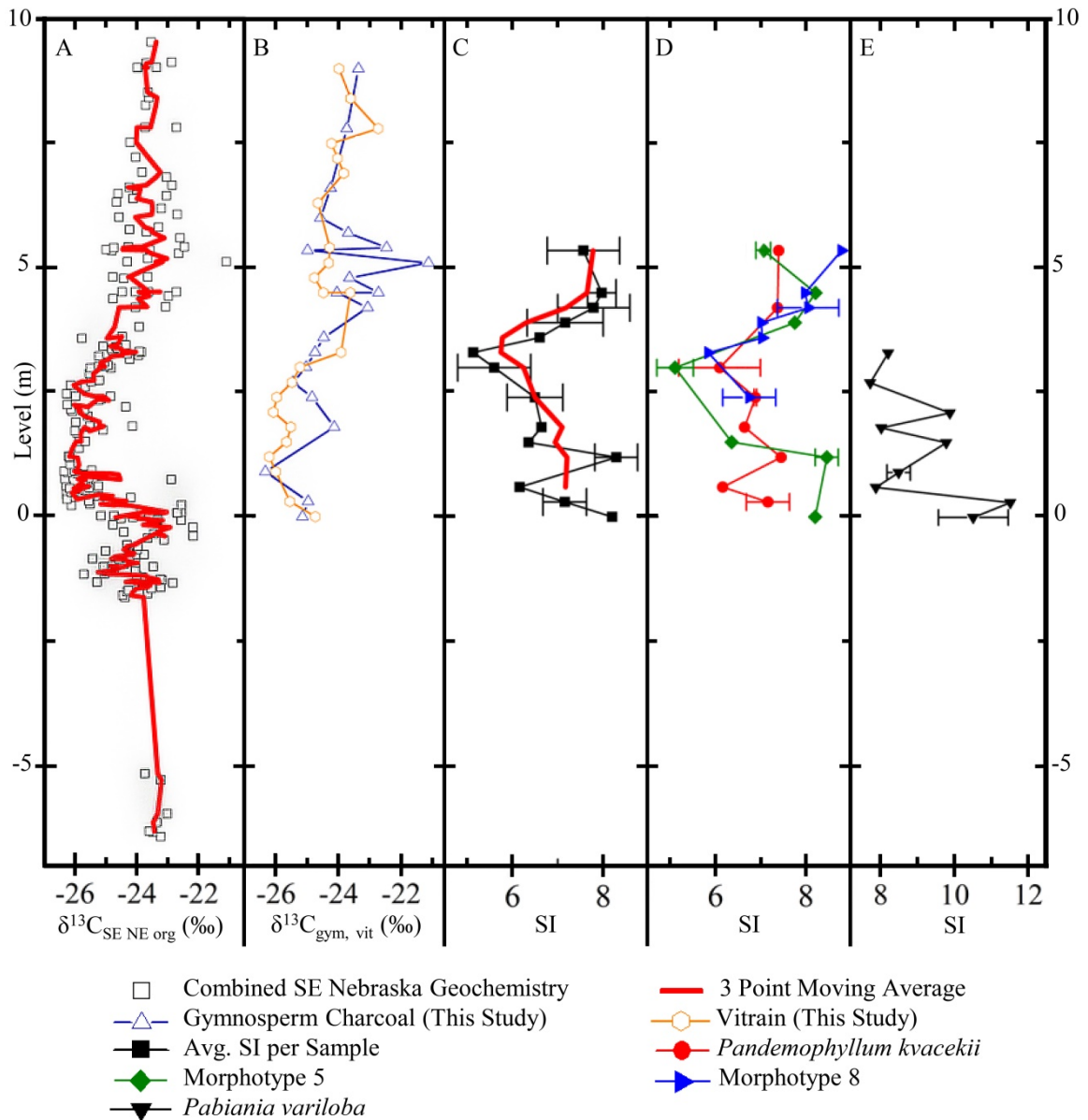


Figure 9: Carbon Isotopes and Stomatal Index from Rose Creek Pit, Southeastern Nebraska. A) Scatterplot of all SE Nebraska geochemistry ($\delta^{13}C_{gym}$, $\delta^{13}C_{vit}$, $\delta^{13}C_{char}$, $\delta^{13}C_{bulk}$; black open boxes). Red line is a 3-point moving average. (Gröcke and Joeckel, 2008; Gröcke et al., 2006). B) $\delta^{13}C_{gym}$ (blue triangles) and $\delta^{13}C_{vit}$ (orange hexagons) from RCP. C) Average SI of all cuticles counted in each sample, excluding *P. variloba* (solid black boxes). Error bars = 1 SD. D) SI from *Pandemophyllum kvacekii* (red circles) and *Pandemophyllum* morphotypes 5 (green diamonds) and 8 (blue right-facing triangles) in each sample. Error Bars = 1 SD. E) SI from *P. variloba* (black downward-facing triangles). Error bars = 1 SD.

well as the brief increases in SI during the overall trend of decrease, and the following rise in SI values as $\delta^{13}\text{C}$ returns to pre-excursion values is seen in *P. kvacekii*, the *Pandemophyllum* morphotypes and *P. variloba* SI curves (Figs. 9D–E). However, subtle differences exist between the SI curves, particularly when the *Pandemophyllum* morphotypes are compared to *P. variloba*.

As stated, after the initial drop in SI low in the RCP section, SI briefly rises back to values approximately equal to those at 0 m (Fig. 9C). This is seen in *P. kvacekii* and morphotype 5, which are the only *Pandemophyllum* morphotypes found from 0–2.4 m (Fig. 9D). In *P. variloba*, SI initially rises slightly from ~10.51 to ~11.51, and then shows a much greater decrease in SI values (to ~7.86) than the *Pandemophyllum* morphotypes (Fig. 9E). *Pabiania* also shows the increase in values (to ~8.48) following the initial decrease, but does not increase back to the values at 0 m like the *Pandemophyllum* morphotypes (Figs. 9D–E). In addition, while the *Pandemophyllum* morphotypes continue to decrease throughout the negative excursion, *P. variloba* shows a second increase in SI values to ~8.01 (Figs. 9D–E). All three *Pandemophyllum* morphotypes show the return to values similar to those low in the section as $\delta^{13}\text{C}$ returns to pre-excursion values (Fig. 9D). No *P. variloba* samples were isolated above 3.6 m in the section, so the return to higher values is not captured (Fig. 9E).

At 0 m in the RCP section (i.e. the approximate beginning of the negative excursion), the Barclay et al. (2010) *L. nobilis* (Eq. 5) transfer function gives an inferred CO_2 level of 437 ppm ($\pm 95\%$ CI [Eq. 7–8] = 391–490 ppm) and the *H. zenkeri* (Eq. 6) transfer function gives an inferred CO_2 level of 334 ppm ($\pm 95\%$ CI [Eq. 9–10] = 330–372 ppm) (Fig. 10B). The Kürschner et al. (2008) *L. pseudoprinceps* (Eq. 4) gives

Carbon Isotopes and pCO₂ from Rose Creek Pit, Southeastern Nebraska

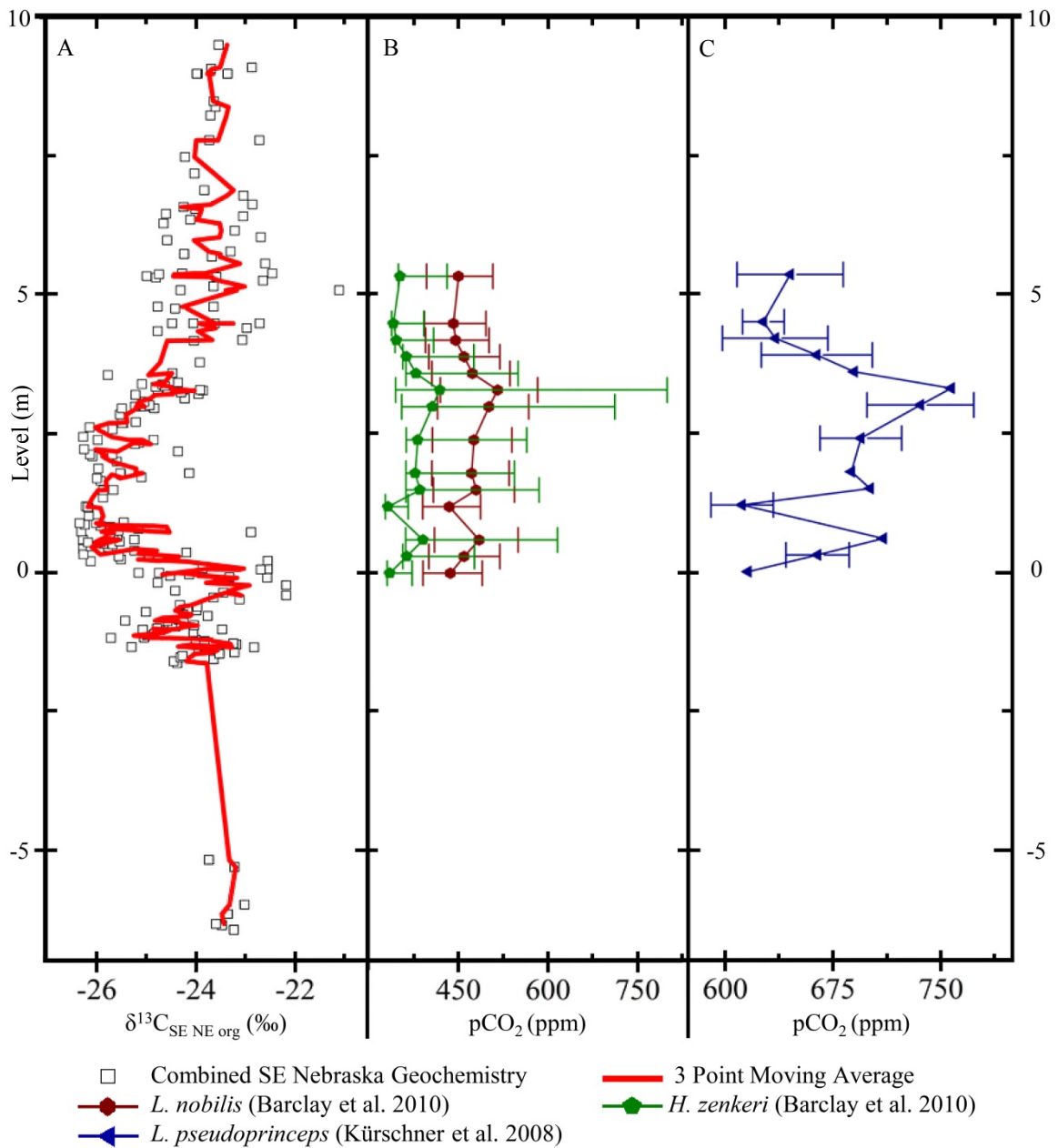


Figure 10: Carbon Isotopes and pCO₂ from Rose Creek Pit, Southeastern Nebraska. A) Scatterplot of all SE Nebraska geochemistry ($\delta^{13}\text{C}_{\text{Char}}$, $\delta^{13}\text{C}_{\text{Vit}}$, $\delta^{13}\text{C}_{\text{Bulk}}$; black open boxes). Red line is a 3-point moving average (Gröcke and Joeckel, 2008; Gröcke et al., 2006). B) pCO₂ estimates from transfer functions derived by Barclay et al. (2010) from extant lauraceous species *Laurus nobilis* (maroon hexagons) and *Hypodaphnis zenkeri* (green pentagons). Error bar = 95% CI equations also derived by Barclay et al. (2010). C) pCO₂ estimates from a transfer function derived by Kürschner et al. (2008) from the extinct lauraceous species *Laurophyllum pseudoprinceps* cross calibrated with Miocene CO₂ inferred from three extant species (*Laurus abchasica*, *Ocotea hradekensis*, and *Ginkgo biloba*). Error bars = SI plus SD (in samples SD was calculated) used in the *L. pseudoprinceps* equation.

an inferred CO₂ level of 616 ppm (Fig. 10C). At the end of the negative excursion (~3.3 m), CO₂ levels reach their highest value. The Barclay et al. (2010) *L. nobilis* transfer function gives an inferred CO₂ level of 515 ppm ($\pm 95\%$ CI = 419–582 ppm) and the *H. zenkeri* transfer function gives an inferred CO₂ level of 419 ppm ($\pm 95\%$ CI = 345–800 ppm) (Fig. 10B). The Kürschner et al. (2008) *L. pseudoprinceps* gives an inferred CO₂ level of 757 ppm. CO₂ responds to the return to pre-excursion values (~4.5 m) by, likewise, returning to the approximate values seen at 0 m (Fig. 10C). The Barclay et al. (2010) *L. nobilis* transfer function gives an inferred CO₂ level of 441 ppm ($\pm 95\%$ CI = 393–496 ppm) and the *H. zenkeri* transfer function gives an inferred CO₂ level of 340 ppm ($\pm 95\%$ CI = 338–392 ppm) (Fig. 10B). The Kürschner et al. (2008) *L. pseudoprinceps* gives an inferred CO₂ level of 626 ppm (SI \pm SD = 612–641 ppm) (Fig. 10C). Finally, at the level of the lignite, CO₂ increases slightly. The Barclay et al. (2010) *L. nobilis* transfer function gives an inferred CO₂ level of 450 ppm ($\pm 95\%$ CI = 397–508 ppm) and the *H. zenkeri* transfer function gives an inferred CO₂ level of 352 ppm ($\pm 95\%$ CI = 349–431 ppm) (Fig. 10B). The Kürschner et al. (2008) *L. pseudoprinceps* gives an inferred CO₂ level of 645 ppm (SI \pm SD = 608–682 ppm) (Fig. 10C).

IV. DISCUSSION

The $\delta^{13}\text{C}_{\text{gym}}$ and $\delta^{13}\text{C}_{\text{vit}}$ curves generated in this study match the $\delta^{13}\text{C}_{\text{char}}$ and $\delta^{13}\text{C}_{\text{bulk}}$ curves of Gröcke et al. (2006), the $\delta^{13}\text{C}_{\text{bulk}}$ curves generated from sediment cores (RCP UC and Core 13A05) of Gröcke and Joeckel (2008) (Fig. 8E), and the $\delta^{13}\text{C}_{\text{foram}}$ curve of Wilson and Norris (2001) (Fig. 8G). The $\delta^{13}\text{C}_{\text{char}}$ and $\delta^{13}\text{C}_{\text{vit}}$ curves capture the negative excursion seen in the $\delta^{13}\text{C}_{\text{char}}$ and $\delta^{13}\text{C}_{\text{bulk}}$ curves from RCP and surrounding areas (Fig. 8E) (Gröcke and Joeckel, 2008; Gröcke et al., 2006), as well as marine $\delta^{13}\text{C}$ curves from bulk rock/carbonate (Fig. 8G) (Bornemann et al., 2005; Phelps, 2012; Reichelt, 2005; Watkins et al., 2005; Wilson and Norris, 2001). This, along with the work of many other researchers (see the “Fossil Charcoal, Vitrain, and Carbon Isotopes” sub-section in chapter I), verifies the original assertion of Scholle and Arthur (1980) that $\delta^{13}\text{C}$ excursions recorded in marine carbonate could be communicated to land plants through changes in $\delta^{13}\text{C}_{\text{atm}}$. Furthermore, the gradual return to pre-excursion values is captured (Fig. 8E). I was able to recover charcoal and vitrain samples at position of paleosol, located between 6.6–8.6 m in the Gröcke et al. (2006) section. These show a $\delta^{13}\text{C}$ comparable to that of underlying samples that post-date the negative excursion.

SI from RCP cuticle (*P. kvacekii*, *P. variloba*, and related morphotypes) (Figs. 9C–E) and atmospheric CO_2 (Figs. 10B–C) correspond to changes in $\delta^{13}\text{C}$ in the general manner found by other researchers (Barclay et al., 2010; McElwain et al., 2005). During the negative $\delta^{13}\text{C}$ excursion, SI decreases and CO_2 gradually increases, indicating an increase in the amount of atmospheric carbon during the release of isotopically-light carbon. This is most likely due CO_2 and CH_4 from the concurrent eruption of a LIP, the

central Kerguelen Plateau (100–101 Myr). SI returns to pre-excursion values in parallel with $\delta^{13}\text{C}$. One issue with the CO_2 inferred from the transfer functions of Barclay et al. (2010) (Eqs. 5–10) and Kürschner et al. (2008) (Eq. 4) is that they are based on herbarium specimens of extant species of Lauraceae, which have been exposed to CO_2 levels of ~180–280 ppm for the last 800,000+ years, and do not include plants grown in chambers at elevated CO_2 (Petit et al., 1999). This makes it unlikely that they will be able to predict CO_2 levels in the mid-Cretaceous, when inferred CO_2 levels could have been as high as ~1800 ppm (Bernier, 1998; Breecker et al., 2010; Royer, 2010). For instance, with the anomalously low SI of 1, the transfer function of Kürschner et al. (2008) gives a CO_2 of 947 ppm, well below the high end of estimates at or near the ACB. Looking at the estimates for the ACB in this study, the highest CO_2 estimate of 800 ppm is likewise well below the high end of estimates at the ACB. In the future, I plan to improve the existing transfer functions with data from lauraceous plants grown at high CO_2 .

Gröcke et al. (2006) proposed that the inferred depositional hiatus at RCP was responsible for the absence of the positive isotopic shift found in other studies of OAE1d (Bornemann et al., 2005; Erbacher et al., 1996; Leckie et al., 2002; Nederbragt et al., 2001; Reichelt, 2005; Robinson et al., 2008; Scott et al., 2013; Stoll and Schrag, 2000; Strasser et al., 2001; Watkins et al., 2005; Wilson and Norris, 2001). However, in the interval above the negative excursion and below the paleosol and the inferred position of the ACB, seven slightly enriched values (avg. = 0.66‰) were found in $\delta^{13}\text{C}_{\text{gym}}$, $\delta^{13}\text{C}_{\text{char}}$, and $\delta^{13}\text{C}_{\text{bulk}}$ in the interval from 4.41–6.64 m, both in this study and Gröcke et al. (2006) (Fig. 8D). One $\delta^{13}\text{C}_{\text{gym}}$ sample at 5.1 m gave a significantly enriched value (~2.21‰).

The relatively tight clustering (six of the eight enriched values occur 4.5–5.58 m) suggests that this might represent the positive phase of the isotopic excursion during OAE1d. However, in the same interval there are many $\delta^{13}\text{C}$ values that are equal to or slightly more negative than pre-excursion values. If sedimentation rates are relatively constant, and the negative excursion covers ~3.3 m, then the much longer positive excursion at RCP would be expected to be many meters thick.

It is possible that some unknown environmental factor is either hiding the expression of the positive excursion or causing the enriched values in the RCP section. One possibility is that the charcoal and vitrain from the interval of the enriched values represents closed canopy vegetation using respired CO_2 . This could cause: 1) more negative values that might reduce or hide positive values (Van der Merwe and Medina, 1989), or 2) $\delta^{13}\text{C}$ values to vary by up to 6‰, which could explain the slightly negative and slightly positive swings in the interval (Graham and Freeman, 2013). Another environmental factor of concern is an increase in salinity. Increased salinity could cause a positive $\delta^{13}\text{C}$ shift and could be responsible for the enriched values, though homogenized gymnosperm charcoal was used in this study to counteract this effect (Guy et al., 1980; Hasegawa, 2003). In addition, increased salinity would be at odds with the regression event beginning ~0.5 Myr before the ACB that was evoked by Gröcke et al. (2006) to explain the depositional hiatus (Haq et al., 1987). In the absence of an obvious environmental factor, CO_2 , inferred from SI, could give a possible location of the positive excursion at RCP, or possibly give insight into source of the positive values.

Among the samples that were restricted to a width of 2.5 cm, no cuticle samples were isolated above 4.5 m in the section, despite the fact that up to 1 kg of material was

processed for these higher samples. However, the lignitic horizon (5.3–5.55 m) at RCP contains abundant cuticle and charcoal (Fig. 8A). This horizon was also not collected using the 2.5 cm thick samples at 30 cm intervals, and instead was collected from the interval of 5–5.35 m. Because of its greater thickness, the sample might average a longer interval of time, assuming similar depositional rates for the clay and lignite. This could explain the large variation in SI of the *Pandemophyllum* morphotypes at that level (*P. kvacekii* = 7.39, morphotype 5 = 7.07, morphotype 8 = 8.71; SD of *Pandemophyllum* morphotypes = 0.8) (Fig. 9D). While morphotype 8 shows the dramatic increase in SI and an inferred decrease in CO₂ that might be expected to coincide with a positive isotopic excursion, both *P. kvacekii* and Morphotype 5 show decreases in SI and corresponding increases in inferred levels of CO₂ (Fig. 9D). Due to this, it is impossible to assess whether the enriched $\delta^{13}\text{C}$ values generated in this study and Gröcke et al. (2006) coincide with significantly higher SI values and lower CO₂ values or are simply the result of some unknown environmental factor.

However, the pattern of changes in SI during the negative $\delta^{13}\text{C}$ excursion and estimates of carbon release, radiative forcing, and temperature change during OAE1d offer a way to compare this event to other carbon cycle perturbations. Barclay et al. (2010) used $\delta^{13}\text{C}$ of terrestrial organics and SI in fossil lauraceous cuticle to infer changes in atmospheric CO₂ at the Cenomanian-Turonian Boundary and OAE2. They found that excursions $\delta^{13}\text{C}$ during OAE2 were accompanied with synchronous changes in atmospheric CO₂, and hypothesized that the pattern of CO₂ change indicated the release of CO₂ via volcanism. The absence of a negative excursion during OAE2 is attributed to the $\delta^{13}\text{C}$ of mantle CO₂, which is approximately equal to that of the atmosphere (pre-

Industrial Revolution $\delta^{13}\text{C}_{\text{atm}} \approx -7\text{‰}$) (Barclay et al., 2010). This event is not directly comparable to OAE1d due to the lack of a negative excursion, but the behavior of atmospheric CO_2 is in line with what has been hypothesized by other researchers (i.e. the positive excursions are accompanied by a drawdown of atmospheric CO_2) (Arthur et al., 1988). In a similar study of changes in SI in various plants and $\delta^{13}\text{C}$ of fossil wood during the TOAE, McElwain et al. (2005) found that the TOAE negative excursion was accompanied by initial rise in SI (decrease in CO_2), followed by a rapid drop in SI values. They hypothesized that this was due to a release of isotopically-light CH_4 and CO_2 due to intrusion of magma from the Karoo-Ferrar LIP of southern Gondwana organic-rich, coal bearing sediments. The pattern of change in SI and CO_2 during this event is comparable to what I have found for OAE1d, though the increase in SI early in the OAE1d excursion is only due to one sample (Fig. 9C). However, the increase in CO_2 during TOAE was much greater (1200 ± 400 ppm) than OAE1d (141–470 ppm).

Estimates of the change in atmospheric carbon during the negative phase of OAE1d are much lower than those estimated from SI for comparable phases during other major carbon cycle perturbations. Siegenthaler and Sarmiento (1993) described the following relationship between increases in atmospheric CO_2 and mass of carbon:

$$1 \text{ ppm } \text{CO}_2 = \sim 2 \text{ gigatons (Gt } [10^{15}\text{g}]) \text{ carbon} \quad [9].$$

Using this relationship and the changes in CO_2 inferred using SI, I estimate that the mass of carbon in the atmosphere during the negative phase of OAE1d increased by $\sim 282\text{--}940$ Gt relative to pre-excursion values. The lower estimate was calculated using the greatest rise in CO_2 inferred from lauraceous transfer functions (141 ppm). The higher estimate was calculated using the greatest possible rise in CO_2 inferred from the 95% CI equations

of Barclay et al. (2010) (470 ppm). It is important to note that due to the limitations of the transfer functions of Barclay et al. (2010) and Kürschner et al. (2008) (Eqs. 4–10), the actual amount of carbon in the atmosphere could have been much larger. In addition, due to increased uptake of carbon by the ocean, soils, and terrestrial biosphere, the increase in the size of the atmospheric reservoir of carbon represents the minimum amount of carbon released.

Wilson and Norris (2001) suggested that the pattern of changes in OAE1d (specifically the geologically brief negative excursion, in particular) was comparable to those of OAE1a and TOAE, which at the time were hypothesized to be caused by methane release (Hesselbo et al., 2000; Jahren and Arens, 1998; Jahren et al., 2001; Opdyke et al., 1999). Jahren et al. (2001) estimated that ~ 300 Gt of carbon was released during OAE1a. However, they treated the atmosphere as a single independent system, had the methane release only affect the atmospheric system, and did not account for changes in the terrestrial biosphere (i.e. changes in photosynthetic productivity, among others). Hesselbo et al. (2000) estimated that approximately 1500–2700 Gt of methane were released during the TOAE, much more than the higher estimate of carbon release presented in this work. Conversely, McElwain et al (2005) estimated that 2,600–4,400 Gt of carbon was added to the atmosphere during TOAE and noted that the estimate of carbon release could be >10,000 Gt if uptake up the oceanic carbon pool was taken into account. However, they concluded that the methane hydrate pool was not large enough to produce a carbon release of that size (McElwain et al., 2005; Milkov, 2004). Beerling et al. (2002a), using a Mass Balance approach, increased the estimate of carbon release during OAE1a to 3000 Gt, and the estimate of release during TOAE to 5000 Gt, 10–16

times higher than the lower estimate for OAE1d and 3–5 times larger than the higher estimate of carbon release presented here for OAE1d. In addition, other major carbon cycle perturbations, though not caused solely by methane, show evidence of much higher levels of carbon release. The Paleocene-Eocene Thermal Maximum is the last known time of widespread ocean anoxia (Dickens et al., 1995). Estimates of carbon released during this event range from 3000–6800 Gt (Panchuk et al., 2008; Zeebe et al., 2009). The bolide impact at the K-T Boundary is resulted in the instantaneous release of 4,600+ Gt of carbon and an increase in atmospheric CO₂ of 2000+ ppm (Beerling et al., 2002b). The data above indicate that OAE1d was a smaller carbon release event than many of the major carbon cycle perturbations of the geologic past.

Estimates of radiative forcing (ΔF) and change in global surface temperature (ΔT_s) from increased CO₂ also indicate that OAE1d was a much smaller event (in terms of global effects) than other major climate cycle perturbations. Radiative Forcing is the measure (in watts per square meter [W/m^2]) of the ability of specific greenhouse gases to restrict long-wave radiation from escaping the atmosphere and returning to space (Parker, 2003). Using estimates of changes in atmospheric CO₂, radiative forcing can be estimated via the following equation,

$$\Delta F = \alpha \ln(C/C_0) \quad [10],$$

where α is a constant (5.35), C is the final concentration of CO₂, and C_0 is the initial concentration of CO₂ (Houghton et al., 2001). Equation 10 gives a $\Delta F \approx 4.74 \text{ W/m}^2$ for the upper estimate of changes in CO₂ (330 ppm to 800 ppm) and $\Delta F \approx 1.1 \text{ W/m}^2$ for the lower estimate of changes in CO₂ (616 ppm to 757 ppm). The lower estimate is

comparable to the estimate of radiative forcing due to anthropogenic CO₂ release during the Industrial Revolution ($\Delta F \approx 1.46 \text{ W/m}^2$).

Estimates of radiative forcing can be used to estimate the change in global temperature during OAE1d via the following equation:

$$\Delta T_s = \lambda \Delta F \quad [11],$$

where λ is climate sensitivity, the response of global temperature to changes in radiative forcing (in units of degrees Kelvin per watts per square meter [K/W/m^2]). Climate sensitivity is normally cited as 0.8 K/W/m^2 . Estimates of change in global temperature produced via equation 11 are in units of Kelvin, but since the scale of Kelvin and Celsius are equal, they can be expressed in Celsius. Using equation 11, I estimate a global temperature increase of $0.88\text{--}3.8 \text{ }^\circ\text{C}$. This is far below estimate of temperature change for other major carbon cycle perturbations based on atmospheric CO₂. Estimates of global temperature increase for the TOAE, K-T Boundary, and PETM range from $5\text{--}8 \text{ }^\circ\text{C}$ or more.

In summation, OAE1d is a global and significant perturbation to the global carbon cycle which had significant effect on marine turnover. It does not, however, appear to be on par with the largest carbon cycle perturbations of the Mesozoic and Cenozoic (i.e. OAE1a, OAE2, TOAE, K-T Boundary, PETM), based estimates of the amount of carbon released and the estimated change in global temperature. The pattern of change in SI and CO₂ (i.e. slow rise in CO₂ throughout the negative excursion) is most likely due to the concurrent eruption of a LIP, the Central Kerguelen Plateau (100–101 Myr). Moving forward, I hope to improve the existing lauraceous transfer functions so that I can refine

estimates of changes in atmospheric CO₂, carbon release, and temperature change during OAE1d.

LITERATURE CITED

2013, Google Earth, Google Inc.

Adobe[®], 2012, Adobe Photoshop[®] CS6.

Ando, A., and Kakegawa, T., 2007, Carbon Isotope Records of Terrestrial Organic Matter and Occurrence of Planktonic Foraminifera from the Albian Stage of Hokkaido, Japan: Ocean-Atmosphere $\delta^{13}\text{C}$ Trends and Chronostratigraphic Implications: *Palaios*, v. 22, no. 4, p. 417–432.

Ando, A., Kakegawa, T., Takashima, R., and Saito, T., 2002, New perspective on Aptian carbon isotope stratigraphy: data from $\delta^{13}\text{C}$ records of terrestrial organic matter: *Geology*, v. 30, no. 3, p. 227–230.

-, 2003, Stratigraphic carbon isotope fluctuations of detrital woody materials during the Aptian Stage in Hokkaido, Japan: Comprehensive $\delta^{13}\text{C}$ data from four sections of the Ashibetsu area: *Journal of Asian Earth Sciences*, v. 21, no. 8, p. 835–847.

Anky-Man, 2014, Wikipedia, The Free Encyclopedia, Wikimedia Foundation, Inc.

Arnold, G. L., Anbar, A. D., Barling, J., and Lyons, T. W., 2004, Molybdenum isotope evidence for widespread anoxia in mid-Proterozoic oceans: *Science*, v. 304, no. 5667, p. 87–90.

Arthur, M. A., Dean, W. E., and Pratt, L. M., 1988, Geochemical and climatic effects of increased marine organic carbon burial at the Cenomanian/Turonian boundary: *Nature*, v. 335, no. 6192, p. 714–717.

- Arthur, M. A., Dean, W. E., and Schlanger, S. O., 1985, Variations in the global carbon cycle during the Cretaceous related to climate, volcanism, and changes in atmospheric CO₂, *in* Sundquist, E. T., and Broecker, W. S., eds., *The Carbon Cycle and Atmospheric CO₂: Natural Variations Archean to Present*, Volume 32, American Geophysical Union, p. 504–529.
- Arthur, M. A., Jenkyns, H. C., Brumsack, H. J., and Schlanger, S. O., 1990, Stratigraphy, geochemistry, and paleoceanography of organic carbon-rich Cretaceous sequences, *Cretaceous Resources, Events and Rhythms: Background and Plans for Research*, Volume 304, p. 75.
- Arthur, M. A., and Sageman, B. B., 1994, Marine Black Shales: Depositional Mechanisms and Environments of Ancient Deposits: *Annual Review of Earth and Planetary Science*, no. 22, p. 499–551.
- Ascough, P. L., Bird, M. I., Wormald, P., Snape, C. E., and Apperley, D., 2008, Influence of production variables and starting material on charcoal stable isotopic and molecular characteristics: *Geochimica et Cosmochimica Acta*, v. 72, no. 24, p. 6090–6102.
- Balesdent, J., Girardin, C., and Mariotti, A., 1993, Site-Related $\delta^{13}\text{C}$ of Tree Leaves and Soil Organic Matter in a Temperate Forest: *Ecology*, v. 74, no. 6, p. 1713–1721.
- Barclay, R. S., McElwain, J. C., and Sageman, B. B., 2010, Carbon sequestration activated by a volcanic CO₂ pulse during Ocean Anoxic Event 2: *Nature Geoscience*, v. 3, p. 205–208.
- Basinger, J. F., and Dilcher, D. L., 1984, Ancient Bisexual Flowers: *Science*, v. 224, no. 4648, p. 511–513.

- Baudin, F., 2005, A Late Hauterivian short-lived anoxic event in the Mediterranean Tethys: the 'Faraoni Event': *Comptes Rendus Geoscience*, v. 337, no. 16, p. 1532–1540.
- Bechtel, A., Markic, M., Sachsenhofer, R. F., Jelen, B., Gratzner, R., Lücke, A., and Püttmann, W., 2004, Paleoenvironment of the upper Oligocene Trbovlje coal seam (Slovenia): *International Journal of Coal Geology*, v. 57, no. 1, p. 23–48.
- Bechtel, A., Sachsenhofer, R. F., Markic, M., Gratzner, R., Lücke, A., and Püttmann, W., 2003, Paleoenvironmental implications from biomarker and stable isotope investigations on the Pliocene Velenje lignite seam (Slovenia): *Organic Geochemistry*, v. 34, no. 9, p. 1277–1298.
- Beerling, D. J., Chaloner, W. G., Huntley, B., Pearson, J. A., and Tooley, M. J., 1993, Stomatal density responds to the glacial cycle of environmental change: *Proceedings of the Royal Society of London. Series B: Biological Sciences*, v. 251, no. 1331, p. 133-138.
- Beerling, D. J., Chaloner, W. G., Huntley, B., Pearson, J. A., Tooley, M. J., and Woodward, F. I., 1992, Variations in the stomatal density of *Salix herbacea* L. under the changing atmospheric CO₂ concentrations of the late- and post-glacial time: *Philosophical Transactions of the Royal Society of London B: Biological Sciences*, v. 336, no. 1277, p. 215–224.
- Beerling, D. J., and Kelly, C. K., 1997, Stomatal Density Responses of Temperate Woodland Plants Over the Past Seven Decades of CO₂ Increase: A Comparison of Salisbury (1927) with Contemporary Data: *American Journal of Botany*, v. 84, no. 11, p. 1572–1583.

- Beerling, D. J., Lomas, M. R., and Gröcke, D. R., 2002a, On the nature of methane gas-hydrate dissociation during the Toarcian and Aptian oceanic anoxic events: *American Journal of Science*, v. 302, no. 1, p. 28–49.
- Beerling, D. J., Lomax, B. H., Royer, D. L., Upchurch Jr., G. R., and Kump, L. R., 2002b, An atmospheric $p\text{CO}_2$ reconstruction across the Cretaceous-Tertiary boundary from leaf megafossils: *Proceedings of the National Academy of Sciences*, v. 99, no. 12, p. 7836–7840.
- Beerling, D. J., McElwain, J. C., and Osborne, C. P., 1998, Stomatal responses of the ‘living fossil’ *Ginkgo biloba* L. to changes in atmospheric CO_2 concentrations: *Journal of Experimental Botany*, v. 49, no. 326, p. 1603–1607.
- Beerling, D. J., and Royer, D. L., 2002, Fossil plants as indicators of the Phanerozoic global carbon cycle: *Annual Review of Earth and Planetary Sciences*, v. 30, no. 1, p. 527–556.
- Beerling, D. J., and Woodward, F. I., 1995, Stomatal responses of variegated leaves to CO_2 enrichment: *Annals of Botany*, v. 75, no. 5, p. 507–511.
- , 1997, Changes in land plant function over the Phanerozoic: reconstructions based on the fossil record: *Botanical Journal of the Linnean Society*, v. 124, no. 2, p. 137–153.
- Benner, R., Fogel, M. L., Sprague, E. K., and Hodson, R. E., 1987, Depletion of ^{13}C in lignin and its implications for stable carbon isotope studies: *Nature*, v. 329, no. 6141, p. 708–710.

- Berner, R. A., 1998, The carbon cycle and carbon dioxide over Phanerozoic time: the role of land plants: *Philosophical Transactions of the Royal Society of London. Series B: Biological Sciences*, v. 353, no. 1365, p. 75–82.
- Bird, M. I., and Ascough, P. L., 2012, Isotopes in pyrogenic carbon: a review: *Organic Geochemistry*, v. 42, no. 12, p. 1529–1539.
- Bird, M. I., Chivas, A. R., and Head, J., 1996, A latitudinal gradient in carbon turnover times in forest soils: *Nature*, v. 381, no. 6578, p. 143–146.
- Bird, M. I., and Gröcke, D. R., 1997, Determination of the abundance and carbon isotope composition of elemental carbon in sediments: *Geochimica et Cosmochimica Acta*, v. 61, no. 16, p. 3413–3423.
- Bird, M. I., Haberle, S. G., and Chivas, A. R., 1994, Effect of altitude on the carbon-isotope composition of forest and grassland soils from Papua New Guinea: *Global Biogeochemical Cycles*, v. 8, no. 1, p. 13–22.
- Bird, M. I., Moyo, C., Veenendaal, E. M., Lloyd, J., and Frost, P., 1999, Stability of elemental carbon in a savanna soil: *Global Biogeochemical Cycles*, v. 13, no. 4, p. 923–932.
- Bird, M. I., Turney, C. S. M., Fifield, L. K., Jones, R., Ayliffe, L. K., Palmer, A., Cresswell, R., and Robertson, S., 2002, Radiocarbon analysis of the early archaeological site of Nauwalabila I, Arnhem Land, Australia: implications for sample suitability and stratigraphic integrity: *Quaternary Science Reviews*, v. 21, no. 8, p. 1061–1075.

- Bornemann, A., Pross, J., Reichelt, K., Herrle, J., Hemleben, C., and Mutterlose, J., 2005, Reconstruction of short-term palaeoceanographic changes during the formation of the Late Albian 'Niveau Breistroffer' black shales (Oceanic Anoxic Event 1d, SE France): *Journal of the Geological Society, London*, v. 162, no. 623–639.
- Breecker, D. O., Sharp, Z. D., and McFadden, L. D., 2010, Atmospheric CO₂ concentrations during ancient greenhouse climates were similar to those predicted for AD 2100: *Proceedings of the National Academy of Sciences*, v. 107, no. 2, p. 576–580.
- Bréhéret, J.-G., 1994, The mid-Cretaceous organic-rich sediments from the Vocontian zone of the French Southeast Basin, *in* Mascle, A., ed., *Hydrocarbon and petroleum geology of France, Volume 4*, Springer–Verlag, p. 295–320.
- Bréhéret, J.-G., and Delamette, M., 1989, Faunal fluctuations related to oceanographical changes in the Vocontian basin (SE France) during Aptian-Albian time: *Geobios*, v. 22, p. 267–277.
- Breistroffer, M., 1937, Sur les niveaux fossilifères de l'Albien dans la fosse vocontienne (Drôme, Hautes-Alpes et Basses Alpes): *Comptes Rendus Hebdomadaires des Seances de l'Academie des Sciences. D: Sciences Naturelles*, v. 204, p. 1492–1493.
- Brenner, R. A., Ludvigson, G. A., Witzke, B. J., Zawistoski, A. N., Kvale, E. P., Ravn, R. L., and Joeckel, R. M., 2000, Late Albian Kiowa-Skull Creek Marine Transgression, Lower Dakota Formation, Eastern Margin of Western Interior Seaway, U.S.A.: *Journal of Sedimentary Research*, v. 70, no. 4, p. 868–878.

- Broadmeadow, M. S. J., Griffiths, H., Maxwell, C., and Borland, A. M., 1992, The carbon isotope ratio of plant organic material reflects temporal and spatial variations in CO₂ within tropical forest formations in Trinidad: *Oecologia*, v. 89, no. 3, p. 435–441.
- Cachier, H., Buat-Ménard, P., Fontugne, M., and Rancher, J., 1985, Source terms and source strengths of the carbonaceous aerosol in the tropics: *Journal of Atmospheric Chemistry*, v. 3, no. 4, p. 469–489.
- Cantino, P. D., Doyle, J. A., Graham, S. W., Judd, W. S., Olmstead, R. G., Soltis, D. E., Soltis, P. S., and Donoghue, M. J., 2007, Towards a phylogenetic nomenclature of Tracheophyta: *Taxon*, v. 56, no. 3, p. 1E–44E.
- Carpenter, K. J., 2005, Stomatal Architecture and Evolution in Basal Angiosperms: *American Journal of Botany*, v. 92, no. 10, p. 1595–1615.
- Ceulemans, R., Van Praet, L., and Jiang, X. N., 1995, Effects of CO₂ enrichment, leaf position and clone on stomatal index and epidermal cell density in poplar (*Populus*): *New Phytologist*, v. 131, no. 1, p. 99–107.
- Chen, L.-Q., Li, C.-S., Chaloner, W. G., Beerling, D. J., Sun, Q.-G., Collinson, M. E., and Mitchell, P. L., 2001, Assessing the Potential for the Stomatal Characters of Extant and Fossil *Ginkgo* Leaves to Signal Atmospheric CO₂ Change: *American Journal of Botany*, v. 88, no. 7, p. 1309–1315.
- Clarke, L. J., and Jenkyns, H. C., 1999, New oxygen isotope evidence for long-term Cretaceous climatic change in the Southern Hemisphere: *Geology*, v. 27, no. 8, p. 699–702.

- Cleal, C. J., James, R. M., and Zodrow, E. L., 1999, Variation in stomatal density in the Late Carboniferous gymnosperm frond *Neuropteris ovata*: *Palaios*, v. 14, no. 2, p. 180–185.
- Clifford, S., Black, C., Roberts, J., Stronach, I., Singleton-Jones, P., Mohamed, A., and Azam-Ali, S., 1995, The effect of elevated atmospheric CO₂ and drought on stomatal frequency in groundnut (*Arachis hypogaea* (L.)): *Journal of Experimental Botany*, v. 46, no. 7, p. 847–852.
- Coccioni, R., and Galeotti, S., 2003, The mid-Cenomanian Event: prelude to OAE 2: *Palaeogeography, Palaeoclimatology, Palaeoecology*, no. 190, p. 427–440.
- Cohen-Ofri, I., Weiner, L., Boaretto, E., Mintz, G., and Weiner, S., 2006, Modern and fossil charcoal: aspects of structure and diagenesis: *Journal of Archaeological Science*, v. 33, no. 3, p. 428–439.
- Czimczik, C. I., Preston, C. M., Schmidt, M. W. I., Werner, R. A., and Schulze, E.-D., 2002, Effects of charring on mass, organic carbon, and stable carbon isotope composition of wood: *Organic Geochemistry*, v. 33, no. 11, p. 1207–1223.
- Czimczik, C. I., Schmidt, M. W. I., and Schulze, E.-D., 2005, Effects of increasing fire frequency on black carbon and organic matter in Podzols of Siberian Scots pine forests: *European Journal of Soil Science*, v. 56, no. 3, p. 417–428.
- DeNiro, M. J., and Hastorf, C. A., 1985, Alteration of ¹⁵N/¹⁴N and ¹³C/¹²C ratios of plant matter during the initial stages of diagenesis: Studies utilizing archaeological specimens from Peru: *Geochimica et Cosmochimica Acta*, v. 49, no. 1, p. 97–115.
- Diaz, R. J., and Rosenberg, R., 2008, Spreading dead zones and consequences for marine ecosystems: *Science*, v. 321, no. 5891, p. 926–929.

- Dickens, G. R., O'Neil, J. R., Rea, D. K., and Owen, R. M., 1995, Dissociation of oceanic methane hydrate as a cause of the carbon isotope excursion at the end of the Paleocene: *Paleoceanography*, v. 10, no. 6, p. 965–971.
- Eckmeier, E., Gerlach, R., Skjemstad, J. O., Ehrmann, O., and Schmidt, M. W. I., 2007, Minor changes in soil organic carbon and charcoal concentrations detected in a temperate deciduous forest a year after an experimental slash-and-burn: *Biogeosciences*, v. 4, no. 3, p. 377–383.
- Edwards, D., Kerp, H., and Hass, H., 1998, Stomata in early land plants: an anatomical and ecophysiological approach: *Journal of Experimental Botany*, v. 49, no. Special Issue, p. 255–278.
- Ehleringer, J. R., Lin, Z. F., Field, C. B., Sun, G. C., and Kuo, C. Y., 1987, Leaf Carbon Isotope Ratios of Plants from a Subtropical Monsoon Forest: *Oecologia*, p. 109–114.
- Erba, E., 2004, Calcareous nannofossils and Mesozoic oceanic anoxic events: *Marine Micropaleontology*, v. 52, no. 1, p. 85–106.
- Erba, E., Bartolini, A., and Larson, R., 2004, Valanginian Weissert oceanic anoxic event: *Geology*, v. 32, no. 2, p. 149–153.
- Erbacher, J., Friedrich, O., Wilson, P. A., Birch, H., and Mutterlose, J., 2005, Stable organic carbon isotope stratigraphy across Oceanic Anoxic Event 2 of Demerara Rise, western tropical Atlantic: *Geochemistry, Geophysics, Geosystems*, v. 6, no. 6.

- Erbacher, J., Huber, B. T., Norris, R. D., and Markey, M., 2001, Increased thermohaline stratification as a possible cause for an ocean anoxic event in the Cretaceous period: *Nature*, v. 409, no. 6818, p. 325–327.
- Erbacher, J., and Thurow, J., 1997, Influence of oceanic anoxic events on the evolution of mid-Cretaceous radiolaria in the North Atlantic and western Tethys: *Marine Micropaleontology*, v. 30, no. 1, p. 139–158.
- Erbacher, J., Thurow, J., and Littke, R., 1996, Evolution patterns of radiolaria and organic matter variations: A new approach to identify sea-level changes in mid-Cretaceous pelagic environments: *Geology*, v. 24, no. 6, p. 499–502.
- Estiarte, M., Penuelas, J., Kimball, B. A., Idso, S. B., LaMorte, R. L., Pinter Jr., P. J., Wall, G. W., and Garcia, R. L., 1994, Elevated CO₂ effects on stomatal density of wheat and sour orange trees: *Journal of Experimental Botany*, v. 45, no. 280, p. 1665–1668.
- Farley, M. B., and Dilcher, D. L., 1986, Correlation between Miospores and Depositional Environments of the Dakota Formation (Mid-Cretaceous) of North-Central Kansas and Adjacent Nebraska, U.S.A.: *Palynology*, v. 10, p. 117–133.
- Farquhar, G. D., 1983, On the nature of carbon isotope discrimination in C₄ species: *Australian Journal of Plant Physiology*, no. 10, p. 205–226.
- Farquhar, G. D., Hubick, K. T., Condon, A. G., and Richards, R. A., 1989, Carbon isotope fractionation and plant water-use efficiency, *in* Rundel, P. W., Ehleringer, J. R., and Nagy, K. A., eds., *Stable isotopes in ecological research*, Volume 68, Springer, p. 21–40.

- Farquhar, G. D., and Richards, R. A., 1984, Isotopic composition of plant carbon correlates with water-use efficiency of wheat genotypes: *Functional Plant Biology*, v. 11, no. 6, p. 539–552.
- Ferrio, J. P., Alonso, N., López, J. B., Araus, J. L., and Voltas, J., 2006, Carbon isotope composition of fossil charcoal reveals aridity changes in the NW Mediterranean Basin: *Global Change Biology*, v. 12, no. 7, p. 1253–1266.
- Ferris, R., Long, L., Bunn, S. M., Robinson, K. M., Bradshaw, H. D., Rae, A. M., and Taylor, G., 2002, Leaf stomatal and epidermal cell development: identification of putative quantitative trait loci in relation to elevated carbon dioxide concentration in poplar: *Tree Physiology*, v. 22, no. 9, p. 633–640.
- Ferris, R., Nijs, I., Behaeghe, T., and Impens, I., 1996, Elevated CO₂ and Temperature have Different Effects on Leaf Anatomy of Perennial Ryegrass in Spring and Summer: *Annals of Botany*, no. 78, p. 489–497.
- Friedli, H., Lötscher, H., Oeschger, H., Siegenthaler, U., and Stauffer, B., 1986, Ice core record of the ¹³C/¹²C ratio of atmospheric CO₂ in the past two centuries: *Nature*, v. 324, no. 6094, p. 237–238.
- Gale, A. S., Kennedy, W., Burnett, J., Caron, M., and Kidd, B. E., 1996, The Late Albian to Early Cenomanian succession at Mont Risou near Rosans (Drôme, SE France): an integrated study (ammonites, inoceramids, planktonic foraminifera, nannofossils, oxygen, and carbon isotopes): *Cretaceous Research*, v. 17, no. 5, p. 515–606.

- Giraud, F., Olivero, D., Baudin, F., Reboulet, S., Pittet, B., and Proux, O., 2003, Minor changes in surface-water fertility across the oceanic anoxic event 1d (latest Albian, SE France) evidenced by calcareous nannofossils: *International Journal of Earth Science*, v. 92, no. 267–284.
- Graham, H. V., and Freeman, K. H., Fossil Leaves and Fossil Leaf n-Alkanes: Reconstructing the First Closed Canopied Rainforests, *in Proceedings American Geophysical Union Fall Meeting Abstracts 2013, Volume 1*, p. 02.
- Greenwood, D. R., Scarr, M. J., and Christophel, D. C., 2003, Leaf stomatal frequency in the Australian tropical rainforest tree *Neolitsea dealbata* (Lauraceae) as a proxy measure of atmospheric $p\text{CO}_2$: *Palaeogeography, Palaeoclimatology, Palaeoecology*, v. 196, no. 3, p. 375–393.
- Gröcke, D. R., 1997, Carbon-isotope stratigraphy of terrestrial plant fragments in the Early Cretaceous from south-eastern Australia, *in Wolberg, D. L., Stump, E., and Rosenberg, G. R., eds., Dinofest™ International: Philadelphia, The Academy of Natural Sciences*, p. 457–461.
- , 1998, Carbon-isotope analyses of fossil plants as a chemostratigraphic and palaeoenvironmental tool: *Lethaia*, v. 31, no. 1, p. 1–13.
- Gröcke, D. R., Hesselbo, S. P., and Jenkyns, H. C., 1999, Carbon-isotope composition of Lower Cretaceous fossil wood: Ocean–atmosphere chemistry and relation to sea-level change: *Geology*, v. 27, no. 2, p. 155–158.
- Gröcke, D. R., and Joeckel, R. M., 2008, A stratigraphic test of the terrestrial carbon-isotope record of the latest Albian OAE from the Dakota Formation, Nebraska: *Kansas Geological Survey, Open-File Report.*, v. 2008, no. 2, p. 24–30.

- Gröcke, D. R., Ludvigson, G. A., Witzke, B. J., Robinson, S. A., Joeckel, R. M., Ufnar, D. F., and Ravn, R. L., 2006, Recognizing the Albian-Cenomanian (OAE1d) sequence boundary using plant carbon isotopes: Dakota Formation, Western Interior Basin, USA: *Geology*, v. 34, no. 3, p. 193–196.
- Gröcke, D. R., Price, G. D., Robinson, S. A., Baraboshkin, E. Y., Mutterlose, J., and Ruffell, A. H., 2005, The Upper Valanginian (Early Cretaceous) positive carbon-isotope event recorded in terrestrial plants: *Earth and Planetary Science Letters*, v. 240, no. 2, p. 495–509.
- Guy, R. D., Reid, D. M., and Krouse, H. R., 1980, Shifts in Carbon Isotope Ratios of Two C₃ Halophytes under Natural and Artificial Conditions: *Oecologia*, v. 44, no. 2, p. 241–247.
- Hadley, A., 2010, CombineZP.
- Hakkou, M., Pétrissans, M., Gérardin, P., and Zoulalian, A., 2006, Investigations of the reasons for fungal durability of heat-treated beech wood: *Polymer Degradation and Stability*, v. 91, no. 2, p. 393–397.
- Haq, B. U., Hardenbol, J., and Vail, P. R., 1987, Chronology of fluctuating sea levels since the Triassic: *Science*, v. 235, no. 4793, p. 1156–1167.
- Haq, B. U., and Schutter, S. R., 2008, A chronology of Paleozoic sea-level changes: *Science*, v. 322, no. 5898, p. 64–68.
- Hasegawa, T., 1997, Cenomanian-Turonian carbon isotope events recorded in terrestrial organic matter from northern Japan: *Palaeogeography, Palaeoclimatology, Palaeoecology*, v. 130, no. 1, p. 251–273.

- , 2003, Cretaceous terrestrial paleoenvironments of northeastern Asia suggested from carbon isotope stratigraphy: Increased atmospheric CO₂-induced climate: *Journal of Asian Earth Sciences*, v. 21, no. 8, p. 849–859.
- Hasegawa, T., Pratt, L. M., Maeda, H., Shigeta, Y., Okamoto, T., Kase, T., and Uemura, K., 2003, Upper Cretaceous stable carbon isotope stratigraphy of terrestrial organic matter from Sakhalin, Russian Far East: a proxy for the isotopic composition of paleoatmospheric CO₂: *Palaeogeography, Palaeoclimatology, Palaeoecology*, v. 189, no. 1, p. 97–115.
- Hatcher, P. G., and Clifford, D. J., 1997, The organic geochemistry of coal: from plant materials to coal: *Organic Geochemistry*, v. 27, no. 5, p. 251–274.
- Hatcher, P. G., Wenzel, K. A., and Cody, G. D., Coalification reactions of vitrinite derived from coalified wood, *in* *Proceedings American Chemical Society Symposium Series 1994, Volume 570*, ACS Publications, p. 112–135.
- Hattin, D. E., 1967, Stratigraphic and paleoecologic significance of macroinvertebrate fossils in the Dakota Formation (Upper Cretaceous) of Kansas, *in* Teichert, Curt, and Yochelson, eds., *Essays in paleontology and stratigraphy*, RC Moore Commemorative Volume, Volume 2: Lawrence, Kansas, Kansas University, p. 570–584.
- Haworth, M., Elliott-Kingston, C., and McElwain, J. C., 2011, The stomatal CO₂ proxy does not saturate at high atmospheric CO₂ concentrations: evidence from stomatal index responses of Araucariaceae conifers: *Oecologia*, v. 167, no. 1, p. 11–19.

- Haworth, M., Hesselbo, S. P., McElwain, J. C., Robinson, S. A., and Brunt, J. W., 2005, Mid-Cretaceous $p\text{CO}_2$ based on stomata of the extinct conifer *Pseudofrenelopsis* (Cheirolepidiaceae): *Geology*, v. 33, no. 9, p. 749–752.
- Hays, J. D., and Pitman, W. C., 1973, Lithospheric plate motion, sea level changes and climatic and ecological consequences: *Nature*, v. 246, no. 5427, p. 18–22.
- Heimhofer, U., Hochuli, P. A., Burla, S., Andreson, N., and Weissert, H., 2003, Terrestrial carbon-isotope records from coastal deposits (Algarve, Portugal): a tool for chemostratigraphic correlation on an intrabasinal and global scale: *Terra Nova*, v. 15, no. 1, p. 8–13.
- Heimhofer, U., Hochuli, P. A., Herrle, J. O., and Weissert, H., 2006, Contrasting origins of Early Cretaceous black shales in the Vocontian basin: Evidence from palynological and calcareous nannofossil records: *Palaeogeography, Palaeoclimatology, Palaeoecology*, v. 235, no. 1, p. 93–109.
- Hesselbo, S. P., Gröcke, D. R., Jenkyns, H. C., Bjerrum, C. J., Farrimond, P., Morgans-Bell, H. S., and Green, O. R., 2000, Massive dissociation of gas hydrate during a Jurassic oceanic anoxic event: *Nature*, v. 406, no. 6794, p. 392–395.
- Hesselbo, S. P., Morgans-Bell, H. S., McElwain, J. C., Rees, P. M., Robinson, S. A., and Ross, C. E., 2003, Carbon–Cycle Perturbation in the Middle Jurassic and Accompanying Changes in the Terrestrial Paleoenvironment: *The Journal of Geology*, v. 111, no. 3, p. 259–276.

- Hesselbo, S. P., Robinson, S. A., Surlyk, F., and Piasecki, S., 2002, Terrestrial and marine extinction at the Triassic-Jurassic boundary synchronized with major carbon-cycle perturbation: A link to initiation of massive volcanism?: *Geology*, v. 30, no. 3, p. 251–254.
- Hochuli, P. A., Menegatti, A. P., Weissert, H., Riva, A., Erba, E., and Silva, I. P., 1999, Episodes of high productivity and cooling in the early Aptian Alpine Tethys: *Geology*, v. 27, no. 7, p. 657–660.
- Hoefs, J., 2009, *Stable Isotope Geochemistry*, Springer.
- Hofmann, P., Ricken, W., Schwark, L., and Leythaeuser, D., 2000, Carbon-Sulfur-Iron Relationships and $\delta^{13}\text{C}$ of Organic Matter for Late Albian Sedimentary Rocks from the North Atlantic Ocean: Paleooceanographic Implications: *Palaeogeography, Palaeoclimatology, Palaeoecology*, v. 163, no. 3, p. 97–113.
- Houghton, J. T., Ding, Y., Griggs, D. J., Noguer, M., van der Linden, P. J., Dai, X., Maskell, K., and Johnson, C. A., 2001, *Climate change 2001: the scientific basis*, Cambridge, U. K., Cambridge university press
- Indermühle, A., Stocker, T., Joos, F., Fischer, H., Smith, H., Wahlen, M., Deck, B., Mastroianni, D., Tschumi, J., and Blunier, T., 1999, Holocene carbon-cycle dynamics based on CO_2 trapped in ice at Taylor Dome, Antarctica: *Nature*, v. 398, no. 6723, p. 121–126.
- IPCC, 2007, *Climate change 2007-the physical science basis: Working group I contribution to the fourth assessment report of the IPCC*, Cambridge University Press.

- Jahren, A. H., and Arens, N. C., 1998, Methane hydrate dissociation implicated in Aptian OAE events: Geological Society America Abstracts with Programs, v. 30, p. 53.
- Jahren, A. H., Arens, N. C., Sarmiento, G., Guerrero, J., and Amundson, R., 2001, Terrestrial record of methane hydrate dissociation in the Early Cretaceous: Geology, v. 29, no. 2, p. 159–162.
- Jenkyns, H. C., 1980, Cretaceous Anoxic Events: From Continents to Oceans: Journal of the Geological Society, v. 137, no. 2, p. 171–188.
- , 1988, The early Toarcian (Jurassic) anoxic event; stratigraphic, sedimentary and geochemical evidence: American Journal of Science, v. 288, no. 2, p. 101–151.
- , 2003, Evidence for rapid climate change in the Mesozoic-Palaeogene greenhouse world: Philosophical Transactions of the Royal Society A: Mathematics, Physical, and Engineering Sciences, v. 361, no. 1810, p. 1885–1916; discussion 1916.
- , 2010, Geochemistry of Oceanic Anoxic Events: Geochemistry Geophysics Geosystems, v. 11, no. 3, p. 1–30.
- Joachimski, M., and Buggisch, W., 1993, Anoxic events in the late Frasnian-Causes of the Frasnian-Famennian faunal crisis?: Geology, v. 21, no. 8, p. 675–678.
- Jones, C. E., and Jenkyns, H. C., 2001, Seawater strontium isotopes, oceanic anoxic events, and seafloor hydrothermal activity in the Jurassic and Cretaceous: American Journal of Science, v. 301, no. 2, p. 112–149.
- Jones, M. B., Brown, J. C., Raschi, A., and Miglietta, F., 1995, The effects on *Arbutus unedo* L. of long-term exposure to elevated CO₂: Global Change Biology, v. 1, no. 4, p. 295–302.

- Jones, T. P., and Chaloner, W. G., 1991, Fossil charcoal, its recognition and palaeoatmospheric significance: *Palaeogeography, Palaeoclimatology, Palaeoecology*, v. 97, no. 1, p. 39–50.
- Jones, T. P., Scott, A. C., and Matthey, D. P., 1993, Investigations of “fusain transition fossils” from the Lower Carboniferous: comparisons with modern partially charred wood: *International Journal of Coal Geology*, v. 22, no. 1, p. 37–59.
- Kajiwara, Y., and Kaiho, K., 1992, Oceanic anoxia at the Cretaceous/Tertiary boundary supported by the sulfur isotopic record: *Palaeogeography, Palaeoclimatology, Palaeoecology*, v. 99, no. 1, p. 151–162.
- Kawabe, F., Takashima, R., Wani, R., Nishi, H., and Moriya, K., 2003, Upper Albian to Lower Cenomanian biostratigraphy in the Oyubari area, Hokkaido, Japan: Toward a Cretaceous biochronology for the North Pacific: *Acta Geologica Palona*, v. 53, no. 2, p. 81–91.
- Koch, P. L., Zachos, J. C., and Gingerich, P. D., 1992, Correlation between isotope records in marine and continental carbon reservoirs near the Paleocene Eocene boundary: *Nature*, v. 358, no. 6384, p. 319–322.
- Körner, C., Farquhar, G. D., and Wong, S. C., 1991, Carbon isotope discrimination by plants follows latitudinal and altitudinal trends: *Oecologia*, v. 88, no. 1, p. 30–40.
- Kouwenberg, L. L. R., McElwain, J. C., Kürschner, W. M., Wagner, F., Beerling, D. J., Mayle, F. E., and Visscher, H., 2003, Stomatal Frequency Adjustment of Four Conifer Species to Historical Changes in Atmospheric CO₂: *American Journal of Botany*, v. 90, no. 4, p. 610–619.

- Krull, E. S., Skjemstad, J. O., Graetz, D., Grice, K., Dunning, W., Cook, G., and Parr, J. F., 2003, ^{13}C -depleted charcoal from C_4 grasses and the role of occluded carbon in phytoliths: *Organic Geochemistry*, v. 34, no. 9, p. 1337–1352.
- Kuroda, J., Ogawa, N., Tanimizu, M., Coffin, M., Tokuyama, H., Kitazato, H., and Ohkouchi, N., 2007, Contemporaneous massive subaerial volcanism and late cretaceous Oceanic Anoxic Event 2: *Earth and Planetary Science Letters*, v. 256, no. 1, p. 211–223.
- Kürschner, W. M., 1996, Leaf stomata as biosensors of paleoatmospheric CO_2 levels., LPP Contributions Series, Volume 5: Utrecht, Netherlands, LPP Foundation, p. 1–153.
- , 1997, The Anatomical Diversity of Recent and Fossil Leaves of the Durmast Oak (*Quercus petraea* Lieblein/*Q. pseudocastanea* Goeppert)–Implications for Their Use as Biosensors of Palaeoatmospheric CO_2 Levels: Review of Palaeobotany and Palynology, v. 96, p. 1–30.
- Kürschner, W. M., Kvaček, Z., and Dilcher, D. L., 2008, The Impact of Miocene Atmospheric Carbon Dioxide Fluctuations on Climate and the Evolution of Terrestrial Ecosystems: *Proceedings of the National Academy of Sciences*, v. 105, no. 2, p. 449–453.
- Kürschner, W. M., Stulen, I., Wagner, F., and Kuiper, P. J. C., 1998, Comparison of palaeobotanical observations with experimental data on the leaf anatomy of durmast oak [*Quercus petraea* (Fagaceae)] in response to environmental change: *Annals of Botany*, v. 81, no. 5, p. 657–664.

- Kürschner, W. M., van der Burgh, J., Visscher, H., and Dilcher, D. L., 1996, Oak leaves as biosensors of late Neogene and early Pleistocene paleoatmospheric CO₂ concentrations: *Marine Micropaleontology*, v. 27, no. 1, p. 299–312.
- Kuypers, M. M. M., Pancost, R. D., and Damste, J. S. S., 1999, A large and abrupt fall in atmospheric CO₂ concentration during Cretaceous times: *Nature*, v. 399, no. 6734, p. 342–345.
- Lake, J. A., Quick, W. P., Beerling, D. J., and Woodward, F. I., 2001, Plant Development: Signals from mature to new leaves: *Nature*, v. 411, no. 6834, p. 154.
- Lake, J. A., Woodward, F. I., and Quick, W. P., 2002, Long-distance CO₂ signalling in plants: *Journal of Experimental Botany*, v. 53, no. 367, p. 183–193.
- Larson, R. L., and Erba, E., 1999, Onset of the Mid-Cretaceous greenhouse in the Barremian-Aptian: Igneous events and the biological, sedimentary, and geochemical responses: *Paleoceanography*, v. 14, no. 6, p. 663–678.
- Leavitt, S. W., Donahue, D. J., and Long, A., 1982, Charcoal production from wood and cellulose; implications to radiocarbon dates and accelerator target production: *Radiocarbon*, v. 24, no. 1, p. 27–35.
- Leavitt, S. W., and Long, A., 1982, Evidence for ¹³C/¹²C fractionation between tree leaves and wood: *Nature*, v. 298, no. 5876, p. 742–744.
- , 1986, Stable-carbon isotope variability in tree foliage and wood: *Ecology*, v. 67, no. 4, p. 1002–1010.

- , 1991, Seasonal stable-carbon isotope variability in tree rings: possible paleoenvironmental signals: *Chemical Geology: Isotope Geoscience Section*, no. 87, p. 59–70.
- Leckie, R. M., Bralower, T. J., and Cashman, R., 2002, Oceanic anoxic events and plankton evolution: Biotic response to tectonic forcing during the mid-Cretaceous: *Paleoceanography*, v. 17, no. 3, p. 1–13.
- Lini, A., Weissert, H., and Erba, E., 1992, The Valanginian carbon isotope event: a first episode of greenhouse climate conditions during the Cretaceous: *Terra Nova*, v. 4, no. 3, p. 374–384.
- Lipp, J., Trimborn, P., Fritz, P., Moser, H., Becker, B., and Frenzel, B., 1991, Stable isotopes in tree ring cellulose and climatic change: *Tellus B*, v. 43b, no. 3, p. 322–330.
- Loader, N. J., Robertson, I., and McCarroll, D., 2003, Comparison of stable carbon isotope ratios in the whole wood, cellulose and lignin of oak tree-rings: *Palaeogeography, Palaeoclimatology, Palaeoecology*, v. 196, no. 3, p. 395–407.
- Lomax, B. H., 2001, The use of fossil plants to detect environmental change across the Cretaceous Tertiary Boundary [PhD Dissertation]: University of Sheffield, 240 p.
- López-Horgue, M., Owen, H. G., Rodríguez-Lázaro, J., Orue-Etxebarria, X., Fernandez-Mendiola, P. A., and Garcia-Mondejar, 1999, Late Albian-Early Cenomanian stratigraphic succession near Estella-Lizarra (Navarra, central northern Spain) and its regional and interregional correlation: *Cretaceous Research*, v. 20, no. 4, p. 369–402.

- Ludvigson, G. A., González, L. A., Metzger, R. A., Witzke, B. J., Brenner, R. L., Murillo, A. P., and White, T. S., 1998, Meteoric sphaerosiderite lines and their use for paleohydrology and paleoclimatology: *Geology*, v. 26, no. 11, p. 1039–1042.
- Malone, S. R., Mayeux, H. S., Johnson, H. B., and Polley, H. W., 1993, Stomatal Density and Aperture Length in Four Plant Species Grown Across a Subambient CO₂ Gradient: *American Journal of Botany*, v. 80, no. 12, p. 1413–1418.
- Masiello, C. A., 2004, New directions in black carbon organic geochemistry: *Marine Chemistry*, v. 92, no. 1, p. 201–213.
- Maunu, S. L., 2002, NMR studies of wood and wood products: *Progress in Nuclear Magnetic Resonance Spectroscopy*, v. 40, no. 2, p. 151–174.
- McCarroll, D., and Loader, N. J., 2004, Stable isotopes in tree rings: *Quaternary Science Reviews*, v. 23, no. 7, p. 771–801.
- McElwain, J. C., 1998, Do fossil plants signal palaeoatmospheric CO₂ concentration in the geological past?: *Philosophical Transactions of the Royal Society of London B: Biological Sciences*, v. 353, no. 1365, p. 83–96.
- McElwain, J. C., Beerling, D. J., and Woodward, F. I., 1999, Fossil Plants and Global Warming at the Triassic-Jurassic Boundary: *Science*, v. 285, no. 5432, p. 1386–1390.
- McElwain, J. C., and Chaloner, W. G., 1995, Stomatal Density and Index of Fossil Plants Track Atmospheric Carbon Dioxide in the Palaeozoic: *Annals of Botany*, v. 76, p. 389–395.

- , 1996, The Fossil Cuticle as a Skeletal Record of Environmental Change: *Palaios*, v. 11, no. 4, p. 376–388.
- McElwain, J. C., Mitchell, F. J. G., and Jones, M. B., 1995, Relationship of stomatal density and index of *Salix cinerea* to atmospheric carbon dioxide concentrations in the Holocene: *The Holocene*, v. 5, no. 2, p. 216–219.
- McElwain, J. C., Wade–Murphy, J., and Hesselbo, S. P., 2005, Changes in carbon dioxide during an oceanic anoxic event linked to intrusion into Gondwana coals: *Nature*, v. 435, no. 7041, p. 479–482.
- McParland, L. C., Collinson, M. E., Scott, A. C., Steart, D. C., Grassineau, N. V., and Gibbons, S. J., 2007, Ferns and fires: Experimental charring of ferns compared to wood and implications for paleobiology, paleoecology, coal petrology, and isotope geochemistry: *Palaios*, v. 22, no. 5, p. 528–538.
- Menegatti, A. P., Weissert, H., Brown, R. S., Tyson, R. V., Farrimond, P., Strasser, A., and Caron, M., 1998, High-resolution $\delta^{13}\text{C}$ stratigraphy through the Early Aptian “Livello selli” of the Alpine tethys: *Paleoceanography*, v. 13, no. 5, p. 530–545.
- Meyer, K. M., and Kump, L. R., 2008, Oceanic Euxinia in Earth History: Causes and Consequences: *Annual Review of Earth and Planetary Sciences*, no. 36, p. 251–288.
- Michener, R., and Lajtha, K., 2008, *Stable Isotopes in Ecology and Environmental Science*, Wiley.
- Milkov, A. V., 2004, Global estimates of hydrate-bound gas in marine sediments: how much is really out there?: *Earth-Science Reviews*, v. 66, no. 3, p. 183–197.

- Miyazawa, S.-I., Livingston, N. J., and Turpin, D. H., 2006, Stomatal development in new leaves is related to the stomatal conductance of mature leaves in poplar (*Populus trichocarpa* × *P. deltoides*): *Journal of Experimental Botany*, v. 57, no. 2, p. 373–380.
- Montanez, I. P., Norris, R. D., Algeo, T., Chandler, M. A., Johnson, K. R., Kennedy, M. J., Kent, D. V., Kiehl, J. T., Kump, L. R., and Ravelo, A. C., 2011, *Understanding Earth's Deep Past: Lessons for Our Climate Future*.
- Nederbragt, A. J., Fiorentino, A., and Klosowska, B., 2001, Quantitative analysis of calcareous microfossils across the Albian–Cenomanian boundary oceanic anoxic event at DSDP Site 547 (North Atlantic): *Palaeogeography, Palaeoclimatology, Palaeoecology*, v. 166, no. 3, p. 401–421.
- Neftel, A., Moor, E., Oeschger, H., and Stauffer, B., 1985, Evidence from polar ice cores for the increase in atmospheric CO₂ in the past two centuries: *Nature*, v. 315, no. 6014, p. 45–47.
- O'Leary, M. H., 1981, Carbon isotope fractionation in plants: *Phytochemistry*, v. 20, no. 4, p. 553–567.
- , 1984, Measurement of the isotope fractionation associated with diffusion of carbon dioxide in aqueous solution: *The Journal of Physical Chemistry*, v. 88, no. 4, p. 823–825.
- Opdyke, B. N., Erba, E., Larson, R. L., and Herbert, T., 1999, Hot LIPs, methane, and the carbon record of the Apticore: *Eos Transactions of the American Geophysical Union*, v. 80, no. 46, p. F486–F487.

- Pachauri, R., and Reisinger, A., 2007, *Climate Change 2007: Synthesis Report. Contribution of Working Groups I, II and III to the Fourth Assessment Report of the Intergovernmental Panel on Climate Change: Intergovernmental Panel on Climate Change.*
- Panchuk, K., Ridgwell, A., and Kump, L. R., 2008, Sedimentary response to Paleocene-Eocene Thermal Maximum carbon release: A model-data comparison: *Geology*, v. 36, no. 4, p. 315–318.
- Parker, S. P., 2003, *in* Geller, E., Weil, J., Blumel, D., and Rappaport, A., eds., *McGraw-Hill Dictionary of Scientific and Technical Terms*: New York, NY, McGraw-Hill, p. 2380.
- Passalia, M. G., 2009, Cretaceous $p\text{CO}_2$ estimation from stomatal frequency analysis of gymnosperm leaves of Patagonia, Argentina: *Palaeogeography, Palaeoclimatology, Palaeoecology*, v. 273, no. 1, p. 17–24.
- Pedersen, T. F., and Calvert, S. E., 1990, Anoxia vs. Productivity: What Controls the Formation of Organic-Carbon-Rich Sediments and Sedimentary Rocks?: *American Association Petroleum Geologist Bulletin*, v. 74, no. 4, p. 454–466.
- Penuelas, J., and Matamala, R., 1990, Changes in N and S leaf content, stomatal density and specific leaf area of 14 plant species during the last three centuries of CO_2 increase: *Journal of Experimental Botany*, v. 41, no. 9, p. 1119–1124.

- Petit, J. R., Jouzel, J., Raynaud, D., Barkov, N. I., Barnola, J.-M., Basile, I., Bender, I., Chappellaz, J., Davis, M., Delaygue, G., Delmotte, M., Kotyakov, V. M., Legrand, M., Lipenkov, V. Y., Lorius, C., Pepin, L., Ritz, C., Saltzman, E., and Stievenard, M., 1999, Climate and atmospheric history of the past 420,000 years from the Vostok ice core, *Antarctica: Nature*, v. 399, no. 6735, p. 429–436.
- Petrizzo, M. R., Huber, B. T., Wilson, P. A., and MacLeod, K. G., 2008, Late Albian paleoceanography of the western subtropical North Atlantic: *Paleoceanography*, v. 23, no. 1.
- Phelps, R. M., 2012, Middle-Hauterivian to Lower–Campanian sequence stratigraphy and stable isotope geochemistry of the Comanche Platform, South Texas [PhD Dissertation]: University of Texas at Austin.
- Poole, I., Braadbaart, F., Boon, J. J., and Van Bergen, P. F., 2002, Stable carbon isotope changes during artificial charring of propagules: *Organic Geochemistry*, v. 33, no. 12, p. 1675–1681.
- Poole, I., Weyers, J., Lawson, T., and Raven, J., 1996, Variations in stomatal density and index: implications for palaeoclimatic reconstructions: *Plant Cell and Environment*.
- Pratt, L. M., and King, J. D., 1986, Variable marine productivity and high eolian input recorded by rhythmic black shales in Mid-Cretaceous pelagic deposits from central Italy: *Paleoceanography*, v. 1, no. 4, p. 507–522.
- Preston, C. M., and Schmidt, M. W. I., 2006, Black (pyrogenic) carbon: a synthesis of current knowledge and uncertainties with special consideration of boreal regions: *Biogeosciences*, v. 3, no. 4, p. 397–420.

- Pyne, S. J., Andrews, P. L., and Laven, R. D., 1996, Introduction to Wildland Fire, John Wiley and Sons.
- Qian, Y., Engel, M. H., and Macko, S. A., 1992, Stable isotope fractionation of biomonomers during protokerogen formation: Chemical Geology: Isotope Geoscience Section, v. 101, no. 3, p. 201–210.
- Quan, C., Sun, C., Sun, Y., and Sun, G., 2009, High resolution estimates of paleo-CO₂ levels through the Campanian (Late Cretaceous) based on *Ginkgo* cuticles: Cretaceous Research, v. 30, no. 2, p. 424–428.
- Rasband, W. S., 1997, ImageJ, US National Institutes of Health, Volume 2007.
- Reddy, K. R., Robana, R. R., Hodges, H. F., Liu, X. J., and McKinion, J. M., 1998, Interactions of CO₂ enrichment and temperature on cotton growth and leaf characteristics: Environmental and Experimental Botany, v. 39, no. 2, p. 117–129.
- Reichert, K., 2005, Late Aptian-Albian of the Vocontian Basin (SE-France) and Albian of NE-Texas: Biostratigraphic and paleoceanographic implications by planktic foraminifera faunas [PhD Dissertation]: University of Tubingen.
- Retallack, G. J., 2009, Greenhouse crises of the past 300 million years: Geological Society of America Bulletin, v. 121, no. 9-10, p. 1441–1455.
- Retallack, G. J., and Dilcher, D. L., 1981, Coastal hypothesis for the dispersal and rise to dominance of flowering plants, *in* Niklas, K. J., ed., Paleobotany, Paleoecology, and Evolution, Volume 2: New York, Praeger, p. 27–77.
- Richey, J. D., 2011, Inference of *p*CO₂ Levels during the Late Cretaceous Using Fossil Lauraceae. [Undergraduate Honors Thesis]: Texas State University – San Marcos 39 p.

- Rimmer, S. M., Rowe, H. D., Taulbee, D. N., and Hower, J. C., 2006, Influence of maceral content on $\delta^{13}\text{C}$ and $\delta^{15}\text{N}$ in a Middle Pennsylvanian coal: *Chemical Geology*, v. 225, no. 1, p. 77–90.
- Robinson, S. A., Clarke, L. J., Nederbragt, A., and Wood, I. G., 2008, Mid-Cretaceous oceanic anoxic events in the Pacific Ocean revealed by carbon-isotope stratigraphy of the Calera Limestone, California, USA: *Geological Society of America Bulletin*, v. 120, no. 11–12, p. 1416–1426.
- Robinson, S. A., and Hesselbo, S. P., 2004, Fossil–wood carbon–isotope stratigraphy of the non-marine Wealden Group (Lower Cretaceous, southern England): *Journal of the Geological Society*, v. 161, no. 1, p. 133–145.
- Roeske, C. A., and O'Leary, M. H., 1984, Carbon isotope effects on enzyme-catalyzed carboxylation of ribulose biphosphate: *Biochemistry*, v. 23, no. 25, p. 6275–6284.
- Rowson, J. M., 1943, The significance of stomatal index as a differential character: *Quarterly Journal of Pharmacy and Pharmacology*, v. 16, no. 3, p. 255–263.
- Royer, D. L., 2001, Stomatal density and stomatal index as indicators of paleoatmospheric CO_2 concentration: *Review of Palaeobotany and Palynology*, v. 114, no. 1, p. 1–28.
- Royer, D. L., 2003, Estimating Latest Cretaceous and Tertiary Atmospheric CO_2 from Stomatal Indices, *in* Wing, S. L., ed., *Special Papers-Geological Society of America Volume 369*, Geological Society of America, p. 79–93.
- , 2010, Fossil soils constrain ancient climate sensitivity: *Proceedings of the National Academy of Sciences*, v. 107, no. 2, p. 517–518.

- Royer, D. L., Wing, S. L., Beerling, D. J., Jolley, D. W., Koch, P. L., Hickey, L. J., and Berner, R. A., 2001, Paleobotanical evidence for near present-day levels of atmospheric CO₂ during part of the Tertiary: *Science*, v. 292, no. 5525, p. 2310–2313.
- Rundgren, M., and Beerling, D. J., 1999, A Holocene CO₂ record from the stomatal index of subfossil *Salix herbacea* L. leaves from northern Sweden: *The Holocene*, v. 9, no. 5, p. 509–513.
- Salisbury, E. J., 1928, On the Causes and Ecological Significance of Stomatal Frequency, with Special Reference to the Woodland Flora: *Philosophical Transactions of the Royal Society of London B: Biological Sciences, Containing Papers of a Biological Character*, v. 216, no. 431–439, p. 1–65.
- Schlanger, S. O., and Jenkyns, H. C., 1976, Cretaceous Oceanic Anoxic Events: Causes and Consequences: *Geologie en mijnbouw*, v. 55, no. 3–4, p. 179–184.
- Scholle, P. A., and Arthur, M. A., 1980, Carbon isotope fluctuations in Cretaceous pelagic limestones: potential stratigraphic and petroleum exploration tool: *American Association Petroleum Geologist Bulletin*, v. 64, no. 1, p. 67–87.
- Scott, A. C., 1989, Observations on the nature and origin of fusain: *International Journal of Coal Geology*, v. 12, no. 1, p. 443–475.
- , 2000, The Pre-Quaternary history of fire: *Palaeogeography, Palaeoclimatology, Palaeoecology*, v. 164, no. 1, p. 281–329.
- , 2001, Preservation by fire, *in* Briggs, D., and Crowther, P. R., eds., *Palaeobiology II*, John Wiley and Sons, p. 277–280.

- , 2002, Coal petrology and the origin of coal macerals: a way ahead?: International Journal of Coal Geology, v. 50, no. 1, p. 119–134.
- , 2010, Charcoal recognition, taphonomy and uses in palaeoenvironmental analysis: Palaeogeography, Palaeoclimatology, Palaeoecology, v. 291, no. 1, p. 11–39.
- Scott, A. C., and Glasspool, I. J., 2007, Observations and experiments on the origin and formation of inertinite group macerals: International Journal of Coal Geology, v. 70, no. 1, p. 53–66.
- Scott, A. C., and Jones, T. P., 1991a, Fossil charcoal: a plant–fossil record preserved by fire: Geology Today, v. 7, no. 6, p. 214–216.
- , 1991b, Microscopical observations of recent and fossil charcoal: Microscopy and Analysis, v. 24, p. 13–15.
- Scott, R. W., Formolo, M., Rush, N., Owens, J. D., and Oboh-Ikuenobe, F., 2013, Upper Albian OAE 1d event in the Chihuahua Trough, New Mexico, U.S.A: Cretaceous Research, v. 46, p. 136–150.
- Sharma, G. K., and Dunn, D. B., 1968, Effect of environment on the cuticular features in *Kalanchoe fedtschenkoi*: Bulletin of the Torrey Botanical Club, p. 464–473.
- , 1969, Environmental modifications of leaf surface traits in *Datura stramonium*: Canadian Journal of Botany, v. 47, no. 8, p. 1211–1216.
- Siegenthaler, U., and Sarmiento, J. L., 1993, Atmospheric carbon dioxide and the ocean: Nature, v. 365, no. 6442, p. 119–125.

- Sluijs, A., Schouten, S., Pagani, M., Woltering, M., Brinkhuis, H., Damsté, J. S. S., Dickens, G. R., Huber, M., Reichert, G.-J., and Stein, R., 2006, Subtropical Arctic Ocean temperatures during the Palaeocene/Eocene thermal maximum: *Nature*, v. 441, no. 7093, p. 610–613.
- Smith, B. N., and Epstein, S., 1971, Two categories of $^{13}\text{C}/^{12}\text{C}$ ratios for higher plants: *Plant Physiology*, v. 47, no. 3, p. 380–384.
- Steinthorsdottir, M., Jeram, A. J., and McElwain, J. C., 2011, Extremely elevated CO_2 concentrations at the Triassic/Jurassic boundary: *Palaeogeography, Palaeoclimatology, Palaeoecology*, v. 308, no. 3, p. 418–432.
- Stewart, G. R., Turnbull, M. H., Schmidt, S., and Erskine, P. D., 1995, ^{13}C natural abundance in plant communities along a rainfall gradient: a biological integrator of water availability: *Functional Plant Biology*, v. 22, no. 1, p. 51–55.
- Stoll, H. M., and Schrag, D. P., 2000, High-resolution stable isotope records from the Upper Cretaceous rocks of Italy and Spain: Glacial episodes in a greenhouse planet?: *Geological Society of America Bulletin*, v. 112, no. 2, p. 308–319.
- Stott, L. D., Sinha, A., Thiry, M., Aubry, M.-P., and Berggren, W. A., 1996, Global $\delta^{13}\text{C}$ changes across the Paleocene-Eocene boundary: criteria for terrestrial-marine correlations: *Geological Society, London, Special Publications*, v. 101, no. 1, p. 381–399.
- Strasser, A., Caron, M., and Gjermeri, M., 2001, The Aptian, Albian and Cenomanian of Roter Sattel, Romandes Prealps, Switzerland: a high-resolution record of oceanographic changes: *Cretaceous Research*, v. 22, no. 2, p. 173–199.

- Svenson, H., Planke, S., Malthes-Sørensen, A., Jamtveit, B., Myklebust, R., Eidem, T. R., and Rey, S. S., 2004, Release of methane from a volcanic basin as a mechanism for initial Eocene global warming: *Nature*, v. 429, no. 6991, p. 542–545.
- Sverdrup, H. U., Johnson, M. W., and Fleming, R. H., 1942, *The Oceans: Their Physics, Chemistry, and General Biology*, Prentice–Hall New York.
- Takashima, R., Gautam, P., and Nishi, H., 2006, Recent Advances in Research on Terrestrial and Marine sequences from the mid–Cretaceous Oceanic Anoxic Events (OAEs): *Scientific Drilling Journal*, v. 2, p. 50–51.
- Taylor, G. H., Teichmüller, M., Davis, A., Diessel, C. F. K., Littke, R., and Robert, P., 1998, *Organic Petrology*, Stuttgart, Berlin, Gebrüder Borntraeger.
- Thiede, J., Boersma, A., Schmidt, R. R., and Vincent, E., 1981, Reworked fossils in Mesozoic and Cenozoic pelagic central Pacific Ocean sediments, Deep Sea Drilling Project sites 463, 464, 465, and 466, leg 62: Initial Reports of the Deep Sea Drilling Project, v. 62, p. 495–512.
- Thomas, J. F., and Harvey, C. N., 1983, Leaf anatomy of four species grown under continuous CO₂ enrichment: *Botanical Gazette*, v. 144, no. 3, p. 303–309.
- Turgeon, S. C., and Creaser, R. A., 2008, Cretaceous oceanic anoxic event 2 triggered by a massive magmatic episode: *Nature*, v. 454, no. 7202, p. 323–326.
- Turney, C. S. M., Wheeler, D., and Chivas, A. R., 2006, Carbon isotope fractionation in wood during carbonization: *Geochimica et Cosmochimica Acta*, v. 70, no. 4, p. 960–964.

- Upchurch, G. R., and Dilcher, D. L., 1990, Cenomanian Angiosperm Leaf Megafossils, Dakota Formation, Rose Creek Locality, Jefferson County, Southeastern Nebraska: U. S. Geological Survey Bulletin, v. 1915, p. 1–55.
- Van Der Burgh, J., Visscher, H., Dilcher, D. L., and Kürschner, W. M., 1993, Paleoatmospheric signatures in Neogene fossil leaves: *Science*, v. 260, no. 5115, p. 1788–1790.
- Van der Merwe, N. J., and Medina, E., 1989, Photosynthesis and $^{13}\text{C}/^{12}\text{C}$ ratios in Amazonian rain forests: *Geochimica et Cosmochimica Acta*, v. 53, no. 5, p. 1091–1094.
- van Hoof, T. B., Kürschner, W. M., Wagner, F., and Visscher, H., 2006, Stomatal index response of *Quercus robur* and *Quercus petraea* to the anthropogenic atmospheric CO_2 increase: *Plant Ecology*, v. 183, no. 2, p. 237–243.
- Vogel, J. C., 1978, Recycling of carbon in a forest environment: *Oecologia Plantarum*, v. 13, no. 1, p. 89–94.
- Wagner, F., 1998, The influence of environment on the stomatal frequency in *Betula*, LPP Contributions Series, Volume 9: Utrecht, Netherlands, LPP Foundation, p. 1–102.
- Wagner, F., Below, R., De Klerk, P., Dilcher, D. L., Joosten, H., Kürschner, W. M., and Visscher, H., 1996, A natural experiment on plant acclimation: lifetime stomatal frequency response of an individual tree to annual atmospheric CO_2 increase: *Proceedings of the National Academy of Sciences*, v. 93, no. 21, p. 11705–11708.

- Wagner, F., Bohncke, S. J. P., Dilcher, D. L., Kürschner, W. M., van Geel, B., and Visscher, H., 1999, Century-Scale Shifts in Early Holocene Atmospheric CO₂ concentration: *Science*, v. 284, no. 5422, p. 1971–1973.
- Wagner, F., Dilcher, D. L., and Visscher, H., 2005, Stomatal Frequency Responses in Hardwood-Swamp Vegetation from Florida during a 60-Year Continuous CO₂ Increase: *American Journal of Botany*, v. 92, no. 4, p. 690–695.
- Wan, C., Wang, D., Zhu, Z., and Quan, C., 2011, Trend of Santonian (Late Cretaceous) atmospheric CO₂ and global mean land surface temperature: Evidence from plant fossils: *Science China Earth Sciences*, v. 54, no. 9, p. 1338–1345.
- Watkins, D. K., Cooper, M. J., and Wilson, P. A., 2005, Calcareous nannoplankton response to late Albian oceanic anoxic event 1d in the western North Atlantic: *Paleoceanography*, v. 20, no. 2, p. 1–14.
- Weissert, H., Lini, A., Föllmi, K. B., and Kuhn, O., 1998, Correlation of Early Cretaceous carbon isotope stratigraphy and platform drowning events: a possible link?: *Palaeogeography, Palaeoclimatology, Palaeoecology*, v. 137, no. 3, p. 189–203.
- Whiticar, M. J., 1996, Stable isotope geochemistry of coals, humic kerogens and related natural gases: *International Journal of Coal Geology*, v. 32, no. 1, p. 191–215.
- Williams, P. T., and Besler, S., 1996, The influence of temperature and heating rate on the slow pyrolysis of biomass: *Renewable Energy*, v. 7, no. 3, p. 233–250.
- Wilson, P. A., and Norris, R. D., 2001, Warm tropical ocean surface and global anoxia during the mid-Cretaceous period: *Nature*, v. 412, no. 6845, p. 425–429.

- Woodward, F. I., 1986, Ecophysiological studies on the shrub *Vaccinium myrtillus* L. taken from a wide altitudinal range: *Oecologia*, v. 70, no. 4, p. 580–586.
- , 1987, Stomatal numbers are sensitive to increases in CO₂ from pre-industrial levels: *Nature* v. 327, no. 6123, p. 617–618.
- , 1993, Plant Responses to Past Concentrations of CO₂: *Vegetatio*, v. 104-105, p. 145–155.
- Woodward, F. I., and Bazzaz, F. A., 1988, The response of stomatal density to CO₂ partial pressure.: *Journal of Experimental Botany*, v. 39, p. 1771–1981.
- Woodward, F. I., and Kelly, C. K., 1995, The influence of CO₂ concentration on stomatal density: *New Phytologist*, p. 311–327.
- Xiao, B., Sun, X. F., and Sun, R., 2001, Chemical, structural, and thermal characterizations of alkali-soluble lignins and hemicelluloses, and cellulose from maize stems, rye straw, and rice straw: *Polymer Degradation and Stability*, v. 74, no. 2, p. 307–319.
- Zeebe, R. E., Zachos, J. C., and Dickens, G. R., 2009, Carbon dioxide forcing alone insufficient to explain Palaeocene-Eocene Thermal Maximum warming: *Nature Geoscience*, v. 2, no. 8, p. 576–580.